ERDC Letter Report

Environmental Laboratory

US Army Corps of Engineers®
Engineer Research and Development Center

Evaluation of the San Jacinto Waste Pits Feasibility Study Remediation Alternatives

January 2015

Earl Hayter, Paul Schroeder, and Carlos Ruiz

Lower San Jacinto River

9595170

The US Army Engineer Research and Development Center (ERDC) solves the nation's toughest engineering and environmental challenges. ERDC develops innovative solutions in civil and military engineering, geospatial sciences, water resources, and environmental sciences for the Army, the Department of Defense, civilian agencies, and our nation's public good. Find out more at www.erdc.usace.army.mil.

To search for other technical reports published by ERDC, visit the ERDC online library at http://acwc.sdp.sirsi.net/client/default.

Evaluation of the San Jacinto Waste Pits Feasibility Study Remediation Alternatives

Earl Hayter, Paul Schroeder, and Carlos Ruiz

Environmental Laboratory
U.S. Army Engineer Research and Development Center
3909 Halls Ferry Road
Vicksburg, MS 39180-6199

Letter Report

Prepared for U.S. EPA, Region 6
Dallas, TX 75202

Abstract

The U.S. Army Engineer Research and Development Center (ERDC) is providing technical support to the US Environmental Protection Agency (EPA), the goal of which is to prepare an independent assessment of the Potentially Responsible Parties' (PRP) remedial alternative designs for the San Jacinto River Waste Pits Superfund Site, Texas. Specific objectives of this study are the following:

1) Perform an assessment of the design and evaluation of the remediation alternatives presented in the Feasibility Study.
2) Identify other remedial action alternatives or technologies that may be appropriate for the Site.
3) Evaluate the numerical models used by the PRP's modeling contractor for the Site.
4) Assess the hydraulic conditions in and around the San Jacinto River, and utilize surface water hydrologic, hydrodynamic, and sediment transport models appropriate for the Site in performing the assessment.

This is the first of three reports that will be submitted to the EPA, and reports on five of the 20 tasks that were identified by EPA for the ERDC to perform to accomplish the stated goal and objectives.

Contents

Figures and Tables

Figures

Tables

Preface

This study was performed at the request of the U.S. Environmental Protection Agency (EPA) – Region 6 by the Environmental Laboratory (ERDC-EL) of the US Army Corps Engineer Research and Development Center (ERDC), Vicksburg, MS.

At the time of publication, the Deputy Director of ERDC-EL was Dr. Jack Davis and the Director of ERDC-EL was Dr. Elizabeth C. Fleming. Commander of ERDC was COL Jeffrey R. Eckstein. The Director was Dr. Jeffery P. Holland.

Unit Conversion Factors

Multiply	By	To Obtain
feet	0.3048	meters
miles (U.S. nautical)	1,.852	kilometers
miles (U.S. statute)	1.609347	kilometers
acres	4,046.873	Square meters
cubic yards	0.7645549	cubic meters
knots	0.5144444	Meters per second

1 Project Background, Objectives and Tasks

Background

The San Jacinto River Waste Pits Superfund Site (Site) consists of several waste ponds, or impoundments, approximately 14 acres in size, built in the mid-1960s for the disposal of paper mill wastes as well as the surrounding areas containing sediments and soils potentially contaminated by the waste materials that had been disposed of in these impoundments. The impoundments are located immediately north and south of the I-10 Bridge and on the western bank of the San Jacinto River in Harris County, Texas (see Figure 1-1).

Large scale groundwater extraction has resulted in regional subsidence of land in proximity to the Site that has caused the exposure of the contents of the northern impoundments to surface waters. A time-critical removal action was completed in 2011 to stabilize the pulp waste material in the northern impoundments and the sediments within the impoundments to prevent further release of dioxins, furans, and other chemicals of concern into the environment. The removal consisted of placement of a temporary armor rock cap over a geotextile bedding layer and an impermeable geomembrane in some areas. The total area of the temporary armor cap is 15.7 acres. The cap was designed to withstand a 100-year storm event.

The southern impoundments are located south of I-10 and west of Market Street, where various marine and shipping companies have operations (see Figure 1-1). The area around the former southern impoundments is an upland area that is not currently in contact with surface water.

The members of the ERDC-EL Project Delivery Team (PDT) have provided technical assistance to the Site's Remedial Project Manager (RPM) for the past three years that consisted of 1) an evaluation of modeling performed by the modeling contractor for the Potentially Responsible Parties (PRP), 2) an evaluation of the design of the temporary armor cap, and 3) review of the Feasibility Study submitted by the RP.

Figure 1-1 San Jacinto River Waste Pits Superfund Site

Goal and Objectives

The goal of this study is to provide technical support to US Environmental Protection Agency (EPA), including preparing an independent assessment of the PRP's designs and submittals regarding the San Jacinto River Waste Pits Superfund Site. Specific objectives of this study are the following:

1) Perform an assessment of the design and evaluation of the remediation alternatives presented in the Feasibility Study.
2) Identify other remedial action alternatives or technologies that may be appropriate for the Site.
3) Evaluate the numerical models used by the PRP's modeling contractor for the Site.
4) Assess the hydraulic conditions in and around the San Jacinto River, and utilize surface water hydrologic, hydrodynamic, and sediment transport models appropriate for the Site in performing the assessment.

Study Tasks

The following specific tasks were identified by EPA for the PDT to perform to accomplish the stated goal and objectives.

Task 1: Site Visit and Planning Meeting. This task was performed in mid-November.

Task 2: Perform an assessment of the San Jacinto River flow/hydraulic conditions and river bed scour in and around the Site for severe storms, hurricanes, storm surge, etc., using surface water hydrology model(s) appropriate for the Site. In the assessment include an evaluation of potential river bed scour/erosion in light of the historical scour reports for the Banana Bend area and for the San Jacinto River south of the I-10 Bridge.

Task 3: Perform an evaluation of the models and grid cell sizes used by the PRPs for the Site, and include a discussion of any uncertainties in the model results. The evaluation should include a review of the model assumptions regarding bed shear stress, water velocities, and scour.

Task 4: Provide an uncertainty analysis of the model assumptions (flow rates, boundary representation, sediment transport, sedimentation rates, initial bed properties, etc.). Uncertainties should be clearly identified and assessed including sediment loads at the upstream Lake Houston Dam.

Task 5: Perform a technical review of the design and construction of the entire existing cap as it is currently configured. Identify any recommended enhancements to the cap.

Task 6: Assess the ability of the existing cap to prevent migration of dioxin, including diffusion and/or colloidal transport, through the cap with and without the geomembrane/geotextile present.

Task 7: Assess the long-term reliability (500 years) of the cap under the potential conditions within the San Jacinto River, including severe storms, hurricanes, storm surge, subsidence, etc. Include in the assessment an evaluation of the potential for cap failure that may result from waves, prop wash, toe scour and cap undermining, rock particle erosion, substrate material erosion, stream instability, and other potential failure mechanisms. Reliability will be based on the ability of the cap to prevent

any release of contaminated material from the Site. Also discuss any uncertainty regarding the long-term reliability and effectiveness of the existing cap.

Task 8: As part of the cap reliability evaluation, assess the potential impacts to the cap of any barge strikes/accidents from the nearby barge traffic.

Task 9: Identify what institutional/engineering controls (*e.g.*, deed restrictions, notices, buoys, signs, fencing, patrols, and enforcement activities) should be incorporated into the remedial alternatives for the TCRA area and surrounding waters and lands.

Task 10: Identify and document cases, if any, of armoring breaches or confined disposal facility breaches that may have relevance to the San Jacinto site evaluation.

Task 11: Assess the potential amount or range of sediment resuspension and residuals under the various remedial alternatives including capping, solidification, and removal.

Task 12: Identify and evaluate techniques, approaches, Best Management Practices (BMPs), temporary barriers, operational controls, and/or engineering controls (*i.e.*, silt curtains, sheet piles, berms, earth cofferdams, etc.) to minimize the amount of sediment resuspension and sediment residuals concentrations during and after dredging/removal. Prepare a new full removal alternative that incorporates the relevant techniques identified as appropriate.

Task 13: Assess the validity of statements made in the Feasibility Study that the remedial alternative with removal, solidification, and placing wastes again beneath the TCRA cap has great uncertainty as to implementation and that such management of the waste will result in significant releases.

Task 14: Provide a model evaluation of the full removal Alternative 6N identified in the Feasibility Study as well any new alternative(s) developed under Task 12 (Identify and evaluate techniques …) above. Include modeling of sediment resuspension and residuals.

Task 15: Evaluate floodplain management and impact considerations of construction, considering Alternatives 3N, 5aN, 6N, and any new alternative(s) developed under Task 12, in the floodplain and floodwaters pathway and how that would impact flood control, water flow issues and obstructions in navigable waters. This includes impact on changes to potential flooding and any offsets that are needed due to displacement of water caused by construction in the floodway (height or overall footprint) including effects at the current temporary TCRA cap and any potential future remedial measures.

Task 16: Project the long-term (500 years) effects of the capping alternative (3N) compared to the full removal alternative (6N) on water quality.

Task 17: Assess the potential impacts to fish, shellfish, and crabs from sediment resuspension as a result of dredging in the near term and for the long term.

Task 18: Assess the potential for release of material from the waste pits caused by a storm occurring during a removal/dredging operation; identify and evaluate measures for mitigating/reducing any such releases.

Task 19: Estimate the rate of natural attenuation in sediment concentrations/residuals and recommend a monitoring program to evaluate the progress. Discuss the uncertainty regarding the rate of natural attenuation.

Task 20: Assess the appropriateness of the preliminary sediment remediation action level of 220 *ng/kg* in consideration of the appropriate exposure scenario (recreational vs. subsistence fishing), and in consideration of an appropriate Relative Bio-Availability (RBA) factor; and recommend an alternative sediment action level as appropriate.

Study Plan

This first report includes a description of the work performed by the PDT for Tasks 2 - 6. The second report, to be submitted to EPA by 27 February, will describe the work to be performed for Tasks 7 – 14 and 20. The third report, to be submitted to EPA by 10 April, will describe the work to be performed for Tasks 15 – 19. Each of these tasks will be in its own sub-

section of the next Section entitled Project Tasks. The second and third reports will be added to this Letter Report. Each of these three reports will be reviewed by the Site RPM and his team. The final version of the report, which will include the report for all the tasks, will include the revisions directed by the Site RPM.

2 Project Tasks

The report on Tasks 2 – 6 are included in this section.

Task 2

Statement

Perform an assessment of the San Jacinto River (SJR) flow/hydraulic conditions and river bed scour in and around the Site for severe storms, hurricanes, storm surge, etc., using surface water hydrology model(s) appropriate for the Site. In the assessment include an evaluation of potential river bed scour/erosion in light of the historical scour reports for the Banana Bend area and for the SJR south of the I-10 Bridge.

Findings

This task was performed by first reading all identified resources (*e.g.*, reports, journal papers, local sources including newspapers) that describe the hydrologic and hydraulic conditions in the Lower SJR. This information assisted in performing the requested assessment of the SJR hydrodynamic regime. Taking into account the historical scour reports for the Banana Bend area and for the SJR south of the I-10 Bridge, the evaluation of the potential river bed scour/erosion was performed by applying ERDC's LTFATE modeling system to simulate the flood conditions during the October 1994 flood.

Hydrology and Hydrodynamics of the San Jacinto River

The lower SJR is classified as a coastal plain estuary. Dyer (1997) gives the following definition of an estuary: "An estuary is a semi-enclosed coastal body of water which has a free connection to the open sea, extending into the river as far as the limit of tidal influence, and within which sea water is measurably diluted with fresh water derived from land drainage." Land drainage is from the SJR watershed which is a 4,500 square mile area in Harris County, TX. Bedient (2013) reports that this watershed drains an average of approximately two million acre-feet (2.47 km^3) of runoff per year. The SJR connects to Galveston bay which has open connections to the Gulf of Mexico.

The SJR Waste Pits are located in a FEMA designated floodway zone, which is essentially the 100-year floodplain for the SJR. The base flood elevation, which is the water surface elevation resulting from a 100-year flood, for the waste pits has been determined by FEMA to be 19 feet (5.8 m). The low lying Waste Pits are also subject to flooding from storm surges generated by both tropical storms (*i.e.*, hurricanes) and extra-tropical storms. Storm surges generated in the Gulf of Mexico propagate into Galveston Bay and into the Lower SJR. Storm surge modeling conducted by NOAA predicted that category 3 and 5 hurricanes that hit Galveston Bay during high tide would produce surge levels of 23 ft (7.0 m) and 33 ft (10.1 m), respectively, at the Site. In addition, eustatic sea level rise and subsidence also contributes to the vulnerability of the Site. The combined effect of sea level rise and subsidence is reflected in the 1.97 ft (0.6 m) increase in relative sea level rise recorded over the past 100 years in Galveston Bay (Brody *et al.* 2014).

The dynamic nature of the flow regime in the SJR estuary is exemplified by the flood that occurred from October 15-19, 1994. The flood was caused by rainfall that ranged from 8 to more than 28 inches during this five day period and caused severe flooding in portions of 38 counties in southeast Texas (USGS 1995). The 100-year flood was equaled at three of the 43 streamflow gauging stations in the 29 counties that were declared disaster areas after the flow, and it was exceeded at 16 stations. The exceedance of the 100-year flood at the 16 stations ranged from a factor of 1.1 to 2.9 times the 100-year flood. In addition, at 25 of the 43 stations, the peak stages during the flood exceeded the historical maximums (USGS 1995). This flood had a 360,000 ft^3/s (cfs) (10,194 m^3/s (cms)) peak streamflow, 27.0 ft (8.2 m) peak stage, and current velocities greater than 15 ft/s (4.6 m/s) at a gage station on the SJR near Sheldon when up to eight feet of scour was observed in the reach of the SJR south of the I-10 Bridge. The photo on the front cover of this report shows the inundated Site during this flood.

As another example, Hurricane Ike, which was a category 2 hurricane, hit Galveston Bay on September 15, 2008. While this hurricane was less than a 100-year storm, it produced a large storm surge that completely inundated the Site and generated a peak flow rate of 63,100 cfs (1,787 cms) at the Lake Houston Dam. Tropical Storm Allison hit the Galveston Bay

area on June 10, 2001, and generated a peak flow rate at the Lake Houston Dam of 80,500 cfs (2,280 cms).

Evaluation of Potential River Bed Scour

As stated previously, the evaluation of the potential river bed scour/erosion was performed by applying ERDC's LTFATE modeling system to simulate the flood conditions during the October 1994 flood. LTFATE is a multi-dimensional modeling system maintained by ERDC. The hydrodynamic module in LTFATE is the Environmental Fluid Dynamics Code (EFDC) surface water modeling system (Hamrick 2007a; 2007b; and 2007c). EFDC is a public domain, three-dimensional finite difference model that contains dynamically linked hydrodynamic and sediment transport modules. The sediment transport module in LTFATE is the SEDZLJ sediment bed model (Jones and Lick 2001; James *et al.* 2010). A detailed description of LTFATE is given in Appendices A – C. Appendix A contains a general description of the modeling system, Appendix B contains a detailed description of EFDC, and Appendix C contains a description of SEDZLJ. The setup of LTFATE for this estuarine system is described in Task 3.

The hydrodynamic module in LTFATE was used to simulate the time period September 1 – 30, 2008 using the hydrodynamic input files generated by AQ. This simulation produced a hydrodynamic hot start file that was used to simulate the October 1 – 31, 2008 time period during which sediment transport was also simulated. The simulation showed that the Site was completely inundated during this flood (as seen on the photo on the report cover), and that a maximum of 5.8 ft (1.8 m) of scour was predicted to occur in reach of the SJR south of the I-10 Bridge. This simulation was run using only a partially calibrated and validated LTFATE model. Once calibration and validation are complete, the simulation of the September – October time period will be re-run. Updated results (including figures showing the variation in scour and sedimentation depths in proximity to the Site and I-10) will be included in the second report.

Task 3

Statement

Perform an evaluation of the models and grid cell sizes used by the PRPs for the Site, and include a discussion of any uncertainties in the model results. The evaluation should include a review of the model assumptions regarding bed shear stress, water velocities, and scour.

Findings

This task was performed in two steps. The first step consisted of evaluating AQ's models, which included evaluating the impact of the assumptions included in AQ's model framework for their hydrodynamic and sediment transport models, and the second step consisted of setting up ERDC's LTFATE modeling system whose framework does not contain as many assumptions. The second step was performed to quantify the differences between the two modeling systems during select high flow events. As stated previously, LTFATE is described in Appendices A – C. The work performed on this task is described below.

1. Evaluation of AQ's models

The model evaluation process began with the transfer of AQ's model files, including source code, scenario inputs and outputs, and calibration/validation data, and modeling reports to the EPA and the PDT. The review and evaluation of the models included evaluation of model inputs, verification of model code, and benchmarking of model results. More specifically, the methodology used in performing this evaluation was the following:

1. Modeling System Application: Review the application of the AQ models to the SJR estuarine system; specifically evaluate the procedures used to setup, calibrate and validate the models as well as the assumptions included in the AQ model framework.
2. Model Evaluation: a) Evaluate model input files (including model-data comparisons) used for calibration and validation run of both models. b) Verify that the model codes are correctly representing the simulated hydrodynamic and sediment transport processes. c) Benchmark the models by running the models using

the calibration/validation input files and comparing results with those given in AQ's Modeling Report.

Modeling System Application

The applications of the hydrodynamic and sediment transport model components of the AQ modeling system to the SJR are discussed in this section.

The application of AQ's Environmental Fluid Dynamics Code (EFDC) to the SJR model domain was thoroughly reviewed, taking into consideration the constraints of their modeling framework. Specific concerns (the first sentence for each concern is bolded) related to the application of their hydrodynamic and sediment transport models are discussed below.

The location of the downstream boundary of the model domain. As noted by several reviewers, the chosen location required the use of interpolated tidal boundary conditions. EPA's comments to AQ on this subject included the following:

> "The hydraulic regime at the confluence of the Houston Ship Channel at the SJR (Battleship Texas gauge station) is fundamentally different than that which occurs at the mouth of the SJR at Galveston Bay (Morgan's Point gauge station). While approximately symmetrical tidal currents can be expected at both the Battleship Texas and Morgan's Point gauge stations during non-event periods, the symmetry should not exist during periods of flooding. A decoupling of water surface elevations between stations is expected during flood events due to a local heightening of water surface elevation from increased freshwater flow at the mouth of the Houston Ship Channel compared to that of the more tidal-influenced, more open marine environ of Galveston Bay (*e.g.*, Thomann, 1987). Consequently, the water surface elevation response at the downgradient model domain boundary (Battleship Texas) would be significantly different than the water surface elevation response downstream at Galveston Bay (Morgan's Point) during a flood or surge event. As such, the use of data from Morgan's Point may be inappropriate for use in calibrating the subject model."

Regarding this issue, Anchor QEA (2012) states that "sensitivity analysis was conducted to evaluate the effect of using WSE data collected at Morgan's Point on

hydrodynamic and sediment transport model predictions (see Section 4.4)." In Section 4.4 it states the following:

> "Analysis of the effects of data source for specifying WSE at the downstream boundary of the model was accomplished by simulating 2002 using data collected at the Lynchburg gauge station. This year was chosen because it was the only year during which Battleship Texas State Park or Lynchburg WSE data are available and one or more high-flow events (*i.e.*, 2-year flood or greater) occurred. Cumulative frequency distributions of bed elevation changes within the USEPA Preliminary Site Perimeter for the base case and sensitivity simulations are compared on Figure 4-59. Differences in bed elevation change between the two simulations are between -2 and +2 cm over of the bed area in the USEPA Preliminary Site Perimeter (Figure 4-60, bottom panel). A one-to-one comparison of bed elevation changes for each grid cell within the USEPA Preliminary Site Perimeter is presented on Figure 4-60. Overall, the data source for specifying WSE at the downstream boundary of the hydrodynamic model has minimal effect on sediment transport within the USEPA Preliminary Site Perimeter."

The PDT disagrees with the approach used in this analysis of the effects of data source for the WSE. With the differences in the hydrodynamic regimes during floods as described by several of EPA's reviewers, the PDT disagrees with AQ's justification that is based on differences in simulated bed elevation changes within the Site. Just because the differences in bed elevation changes over a one year simulation using the two different WSE data sources were within $\pm$ 2 cm does not indicate that the circulation pattern in the estuary was correctly simulated. If it was not, then the fate of eroded contaminated sediment would be different. As such, the PDT still believes that the more appropriate boundary location would have been in the vicinity of Morgan's Point due to the NOAA tidal station (Number 8770613) at that location. This is where the downstream boundary for the LTFATE model domain was located.

Decoupled hydrodynamic and sediment transport models. The main limitation of AQ's model framework is the use of decoupled hydrodynamic and sediment transport models. This limits its applicability to flow conditions when large morphologic changes (relative to the local flow depth) due to net erosion and net deposition do not occur. Thus, it is not

capable of simulating morphologic changes during large flood events, such as the previously described October 1994 flood. Anchor QEA (2012) states that "model reliability is not significantly affected by not incorporating direct feedback between the hydrodynamic and sediment transport models into the modeling framework, with approximately 8% of the bed area experiencing relative increases or decreases in potential water depth of greater than 20%." However, since these results, *i.e.*, "8% of the bed area …", were obtained using a modeling framework that did not account for changes in bed elevation due to erosion and deposition, which means that those results are in question, they cannot be used to justify not including direct feedback into the modeling framework.

Floodplain areas. Anchor QEA (2012) states that "Floodplain areas (*i.e.*, areas that only get inundated during high flow events) were incorporated into the rectangular numerical grid to adequately represent extreme events in the vicinity of the USEPA Preliminary Site Perimeter." However, more of the floodplain should have been included in other portions of the model grid to correctly represent the flows throughout the estuarine system during the extreme floods simulated during the 21-year model simulation, *e.g.*, the October 1994 flood. The 100-year floodplain was represented in the LTFATE model grid.

Two-Dimensional depth averaged model. It states in Section 2.3 of Anchor QEA (2012) that "the two-dimensional, depth-averaged hydrodynamic model within EFDC was used, which is a valid approximation for the nonstratified flow conditions that typically exist in the San Jacinto River". No salinity data are presented to support this assumption. Stating that models of other estuaries in Texas have used depth-averaged hydrodynamic models is not an acceptable technical justification for this assumption.

Use of hard bottom in the HSC and in the upper reach of the SJR. Regarding this issue, EPA commented that "a justification for assuming the sediment bed was hard bottom in the SJR channel downstream of Lake Houston Dam and in the HSC shall be added to the report. How far downstream in the river channel was a hard bottom assumed? In addition, the report shall comment on potential impacts of these assumptions on sediment and contaminant transport processes in

proximity to the Superfund site." In response, the following text was added to Section 4.2.2:

> ".. the numerical grid was extended up to Lake Houston for hydrodynamic purposes (*i.e.*, to ensure that the tidal prism of the San Jacinto River is properly represented in the model). The sediment bed was specified as hard bottom in this portion of the San Jacinto River because: 1) no significant dioxin bed sources exist within this region (see Section 5.2.5.2); and 2) sparse data were available for specifying bed properties (*i.e.*, there is a large uncertainty in bed type and composition). Thus, specification of the sediment bed in the San Jacinto River channel between the dam and Grennel Slough as cohesive or non-cohesive (*i.e.*, erosion and deposition fluxes were calculated) was not necessary to meet the objectives of this study." This justification seems technically justifiable. However, the discussion of sensitivity analyses results along the San Jacinto River does not take into account the hard bottom assumed for this river between the Lake Houston dam and Grennel Slough. For example, in the second paragraph of Section 5.3.3.2.1 it states "due to flux from sediments [porewater diffusion and erosion]". These processes do not occur to a hard bottom. The appropriate portions of Section 5.3.3.2.1 should have been rewritten (as stated in two previous reviews of this report) to account for the fact that, for example, porewater diffusion, sediment bed mixing, and erosion do not occur in the hard bottom reach. In addition, the procedure used to make "slight adjustments .. to the water column concentrations during calibration to avoid "double counting" of contaminant inputs" needs to be more thoroughly described.

Regarding the hard bottom assumption for the Houston Ship Channel (HSC), the report states the following:

> "With respect to the HSC, specifying the sediment bed as hard bottom was valid because sufficient data were available to specify water column chemical concentrations within the HSC (see Section 5.2.3). It is not necessary to simulate erosion and deposition processes in the HSC because water column chemical concentrations in the HSC can be specified using data, which is all that is necessary for the chemical fate and transport model. Simulating erosion and

deposition fluxes within the HSC would not have improved the predictive capability of the chemical fate and transport model within the USEPA Preliminary Site Perimeter."

These explanations are not justifiable, at least not without quantifying the effects of this assumption using a sensitivity analysis. It states that water column chemical concentration data are available for the HSC. Are there data for all 21 years of the model simulation? While the assumption that "simulating erosion and deposition fluxes within the HSC would not have improved the predictive capability of the chemical fate and transport model within the USEPA Preliminary Site Perimeter" may be valid, a sensitivity test should have been run to quantitatively justify this assumption.

Delineation of the sediment bed. It states in Section 4.2.2 of Anchor QEA (2012) that the sediment bed in a given area was specified as cohesive if the median particle diameter, D_{50}, is less than 250 μm and if the combined clay and silt content is greater than 15 percent. Unless the fraction of clay size sediment is the majority of the combined clay and silt content, it is unlikely if sediment with only these two criteria are cohesive in behavior. More justification needs to be given to support this assumption as it would definitely have an impact on the erosion and transport of sediment in the SJR estuary.

Calibration of the hydrodynamic model. The comparison of measured and simulated depth-averaged velocities shown in Figures 3-23 – 3-25 indicates that the model is under predicting the maximum velocities during both ebb and flood tides, but more so during the latter. In particular, the poor agreement seen during the period July 3 – 4 indicated the model did not accurately represent the combined tidal and riverine flows during this high flow event. The impact that the location of the downstream boundary in the AQ model had on these comparisons is not known. This will be investigated using the LTFATE model. Based on these comparisons of the simulated versus measured velocity times series, I do not completely agree with the last sentence in this section that states 'the calibration and validation results demonstrate that the model is able to simulate the hydrodynamics within the Study Area with sufficient accuracy to meet the objectives of this study'.

Calibration of the sediment transport model. How were the two qualitative conclusions made in the last two sentences of the fourth paragraph of Section 4.3 ("Overall, the model predicts net sedimentation with reasonable accuracy' and 'The general pattern of net sedimentation is qualitatively consistent with known characteristics of the Study Area') arrived at? I come to a different conclusion when examining the comparisons shown in Figs. 4-24 and 4-25, especially for two of the three stations within EPA's Preliminary Site Perimeter. It seems that the model does not predict net sedimentation with reasonable accuracy. My conclusion remains the same even after reading the discussion of the effect of spatial scale on model results in the last paragraph in Sec 4.5. Finally, what are the known characteristics of the Study Area that mentioned in the last sentence?

Other factors/processes not represented in the modeling. These include the following: wind waves and the effects of barges and prop wash on sediment resuspension at the Site. The text that was added to Section 4.1 of Anchor QEA (2012) explaining why wind-wave resuspension is not simulated is valid for non-storm conditions. However, it should have been evaluated in the sensitivity analysis for simulated storm conditions. Regarding the effects of barges and prop wash, it is noted that AQ commented that "The potential effects of ship and barge traffic on sediment transport within the USEPA Preliminary Site Perimeter will be evaluated during the Feasibility Study."

Model Evaluation – Hydrodynamic Model

The AQ hydrodynamic model for the SJR was benchmarked for model output integrity and reliability. These verification and benchmarking tasks were intended to ensure that the hydrodynamic model correctly simulates the riverine and estuarine circulation in the SJR estuary. The evaluation consisted of the following three steps:

1. Model inputs were reviewed to verify consistency with what is documented in Anchor QEA (2012). As a component of this, model-data comparisons were performed for the hydrodynamic input files to insure that the correct parameterizations were used in the model.

2. Model output integrity was verified for selected simulations by recompiling the AQ source code, re-running these simulations with the generated executable, and comparing the model results from these simulations to the model results provided by AQ.

3. Verification of model calculations was accomplished by reviewing model outputs. This review focused on model calculations that were specific to the SJR model domain.

Verification of Model Inputs

Model inputs for bathymetry, inflows, and downstream tidal boundary conditions are based on site-specific data. The goal of the review was to insure the inputs were correctly specified in the model input files. All the hydrodynamic input files were checked, and no problems were identified. Specifically, the input files which described the computational grid were checked to insure the SJR model grid was correctly represented, and the bathymetric data included in the files were correct. Selected model simulation input files, including flow and stage boundary condition files, were also checked for consistency. No inconsistencies were found during these checks, so the model inputs for the hydrodynamic model were successfully verified.

Verification of Model Calculations

The hydrodynamic model for the SJR is based on the EFDC model, which is an open source model supported by EPA Region 4, and which has been applied to many rivers, estuaries, other water bodies worldwide. The AQ version of EFDC was compiled on a Windows computer using the FORTRAN Compiler for Windows by Intel and on a Linux server using the Intel FORTRAN Compiler for LINUX. These recompilations were performed to verify that the AQ version of EFDC could be successfully compiled on different computers using different operating systems (*i.e.*, Windows and Linux). The results obtained using the code executable received from AQ were identical (to within machine precision) with the results obtained using the two recompiled codes. The recompiled code run on the Windows computer was run in full debug mode, but no runtime errors occurred. The conclusion from this task is that the AQ version of EFDC was successfully verified.

Benchmarking of Model Outputs

The 21-year hydrodynamic model simulation was benchmarked to insure that model outputs provided by AQ were reproduced. This simulation was performed using the recompiled code on a Windows computer. The 21-year simulation was successfully completed without any runtime errors, and comparisons of the output from this simulation with that produced using the code executable provided by AQ were identical (to within machine precision). The conclusion from this task is that the AQ version of EFDC was successfully benchmarked.

Model Evaluation - Sediment Transport

The AQ sediment transport model was benchmarked for model output integrity and reliability. These verification and benchmarking tasks were intended to ensure that the sediment transport model correctly simulates the represented sediment transport processes. The evaluation consisted of the following three steps:

1. Model inputs were reviewed to verify consistency with what is documented in Anchor QEA (2012). As a component of this, model-data comparisons were performed for the sediment transport input files to insure that the correct parameterizations were used in this model.

2. The model output integrity was verified for selected simulations by recompiling the AQ source code, re-running these simulations with the generated executable, and comparing the model results from these simulations to the model results provided by AQ.

3. The verification of model calculations was accomplished by reviewing model outputs. This review focused on model calculations that were specific for the SJR modeling system.

Verification of Model Inputs

The following sediment transport model inputs are based on site-specific data, and should be consistent across all model simulations.

- Effective particle diameter for each size class
- Cohesive resuspension parameters (τ_{cr}, A, n)

- *D90* (used for skin friction calculation)
- *D50* (used for initial grain size distribution calculations, as well as other sediment transport calculations)
- Initial grain size distribution
- Dry bulk density

The verification of model inputs for the sediment transport model used consisted of the following components:

1. The values used for the input parameters listed above were reviewed to insure they were within the expected ranges, *i.e.*, ranges of these parameters reported in the literature. The values of all these model inputs used in the sediment transport modeling fell within the expected ranges and/or were the same as given in Anchor QEA (2012).

2. All of the input files for the sediment transport model were checked to verify that the values of the parameters listed above were consistently used. This check revealed that the same values were used for these parameters in all the input files.

3. The time series of solids loading for the sediment transport model were plotted using the model input time series to identify any unusual or outlying solids load inputs. No problems were noted, and the time series were as described in Anchor QEA (2012).

In conclusion, no inconsistencies or incorrect values were found during these checks, so the model inputs for the sediment transport model were successfully verified.

Verification of Model Calculations

The various processes and rate calculations included in the sediment transport model (*e.g.*, settling speed, probability of deposition, resuspension rate) all feed into the computation of the erosion and deposition fluxes for each particle size class in each grid cell at every model time step. Along with velocity and water surface elevation time series for every grid cell that are calculated by the hydrodynamic model, calculated time series of the erosion and deposition fluxes along with the resulting

time series of water column concentrations of suspended sediment in every grid cell are passed to the contaminant transport and fate model. These hydrodynamic and sediment transport time series are used to drive the contaminant model. Considering that the transport and fate of highly hydrophobic chemicals (such as PCBs) that are mostly sorbed to particulate organic matter (POM), and that varying fractions of POM are typically adsorbed to sediment particles, in particular clay and silt size particles, the fate of hydrophobic chemicals are typically governed to a significant degree by the transport and fate of these solids. As such, verification of the calculations of erosion and deposition fluxes of solids in the model is essential.

The calculations of the sediment transport model were checked using the following two tasks:

1. The model code was reviewed to verify that the sediment transport model computes erosion and deposition fluxes correctly.

2. Values of the following parameters and variables that was used in the calculation of erosion and deposition fluxes were printed out during a model run to verify that correct values for the parameters being used in the calculations and that variables (*e.g.*, near-bed suspended sediment concentration) were being calculated correctly.

    a. Deposition flux components: settling speeds of the sediment size classes, probabilities of deposition, and near-bed suspended solid concentrations.

    b. Erosion flux components: critical shear stresses, erosion rate for the non-cohesive solid classes, and the erosion rate for the cohesive size class.

The finding from the first task was that the model code was correctly calculating the specified erosion and deposition fluxes, and the findings from the second task were that a) the correct parameter values were being used, and b) the correct values of relevant variables were being calculated by the model. Therefore, the conclusion from this task is that the sediment

transport related calculations performed by AQ's sediment transport model were successfully verified.

Benchmarking of Model Outputs

The 21-year sediment transport simulation was benchmarked to insure that model outputs provided by AQ were reproduced. This simulation was performed using the recompiled code on a Windows computer. The 21-year simulation successfully finished without any runtime errors, and comparisons of the output with that produced using the code executable provided by AQ were identical (to within machine precision). The preliminary conclusion from this task is that the AQ sediment transport model was successfully benchmarked.

2. Application of LTFATE

Model Setup

Model Domain

The model domain (highlighted in blue) chosen for LTFATE is shown in Figure 2-1. As seen, the downstream boundary is adjacent to Morgan's Point, and includes the 100-year floodplain (FEMA designated floodway zone) as indentified by FEMA.

Model Grid

Figures 2-2 and 2-3 show zoomed in views of the orthogonal curvilinear model grid in proximity to the Site and the downstream boundary at Morgan's Point. The average grid sizes at the Site and at the downstream boundary are 18m by 18m and 50m by 65m, respectively. The average deviation angle from orthogonal for the entire grid is 3.7 degrees, which is acceptable and insures that mass loss of water and transported constituents due to too large a degree of non-orthogonality does not occur.

Bathymetry Data

The same bathymetry data used by AQ (as documented in Appendix A in Anchor QEA (2012) were used in constructing the LTFATE grid.

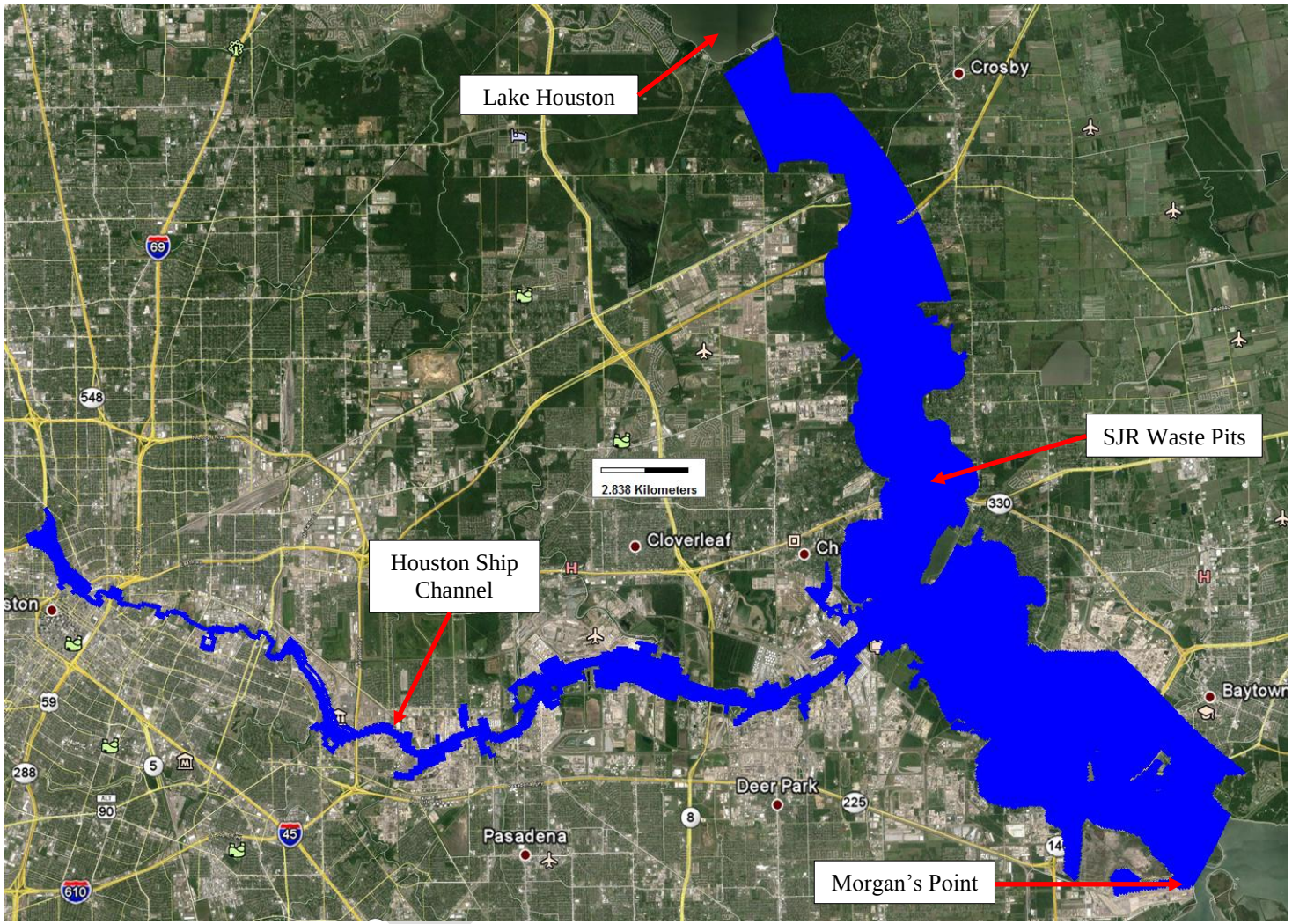

Figure 2-1 LTFATE San Jacinto River Model Domain

Figure 2-2 Grid in Proximity to the SJR Waste Pits Site

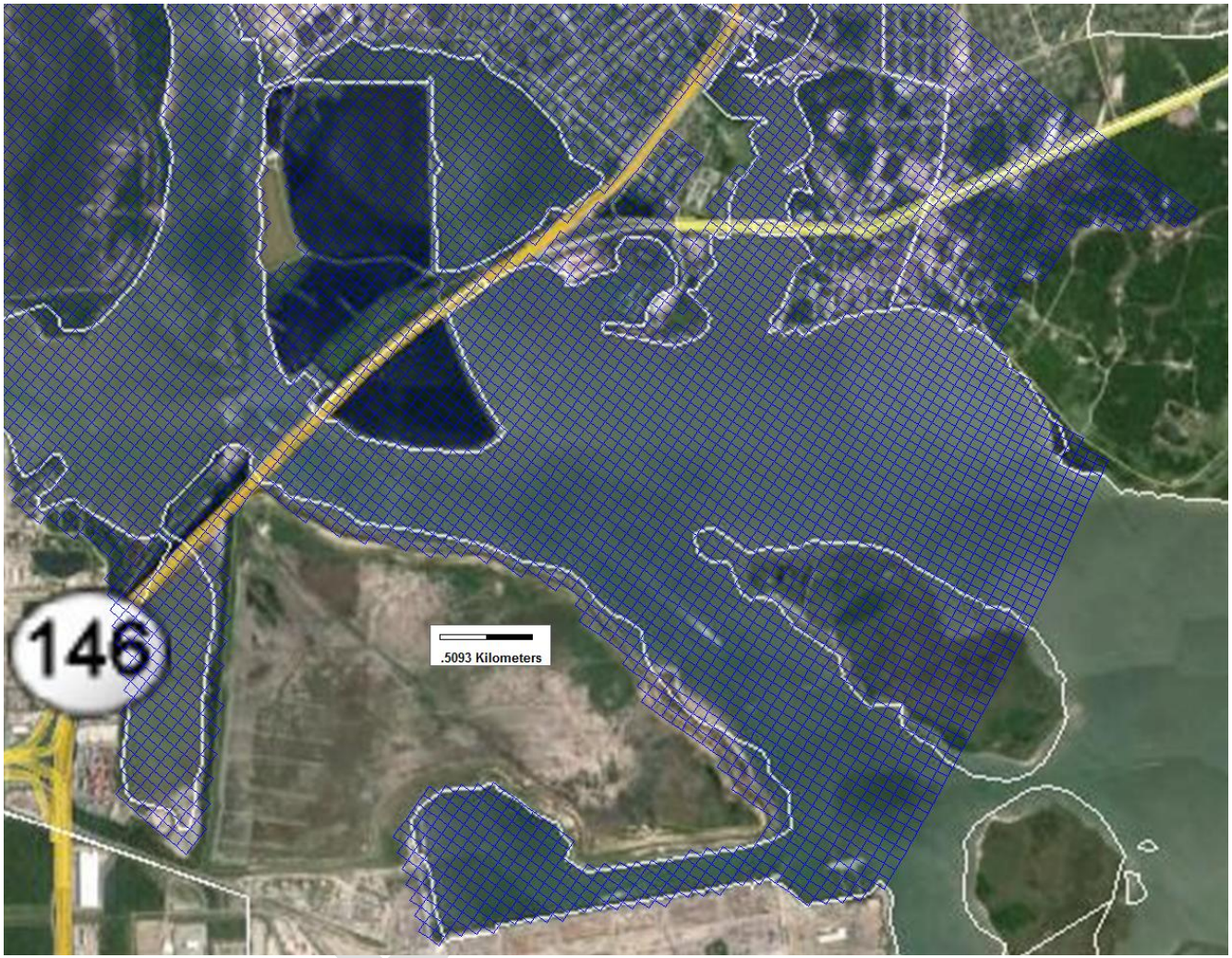

Figure 2-3 Grid in Proximity to the Downstream Boundary

Boundary Conditions

The same boundary conditions used by AQ in their hydrodynamic and sediment transport models were used in LTFATE. The measured water surface elevations at the NOAA tidal station at Morgan's Point were applied to all the wet cells across the downstream open water boundary. The same salinity boundary conditions are used as were used by AQ. Due to the lack of salinity data over the water depth at the downstream boundary, the LFATE model was run in a two-dimensional, depth-averaged mode like AQ's model.

Initial Sediment Bed

In specifying the initial sediment bed, the same four sediment size classes that AQ used were used in the SEDZLJ module in LTFATE. One difference between AQ's version of SEDZLJ and that used in LTFATE is that in the latter, the grid cells are not defined as being either cohesive or noncohesive and then not allowed to change during the model simulation as in the AQ version. In the LTFATE version, whether the surficial sediment is cohesive or noncohesive in behavior is determined for every active (*i.e.*, wet) grid cell during each time step. This enables the changing nature of natural sediment beds due to the varying composition of suspended sediment as well as sediment being transported as bedload to be represented. It was assumed that floodplain cells have an initial hard bottom, *i.e.*, they cannot erode. However, sediment is allowed to deposit on inundated floodplain cells, and the deposited sediment is allowed to resuspend if the bed surface of these cells is subjected to a high enough bed shear stress while the floodplain cell is wet. This is also different from the methodology used by AQ as their model does not allow sediment being carried in suspension to deposit on cells (whether they are floodplain or wet cells) that have a hard bottom.

Model Debugging

To insure that both the hydrodynamic and sediment transport modules in LTFATE were setup correctly, the model was run in full debug mode (Using the Intel FORTRAN compiler) for three days. The reason that it was run for only three days is that the compile code runs much slower in debug mode than it does in optimized mode.

Simulated Processes

The differences between LTFATE and AQ's sediment transport model are the following: 1) Bedload transport is simulated in LTFATE but not in AQ's sediment transport model; 2) The effect of bottom slope on bedload transport and erosion rates is accounted for in LTFATE but not in AQ's sediment transport model. The methodology described by Lick (2009) to include the effect of bed slope on erosion rates and bedload transport is incorporated in the LTFATE version of SEDZLJ. The bed slopes in both the x- and y-directions are calculated, and scaling factors are applied to the bed shear stress, erosion rate, and bedload transport equations. A maximum adverse bed slope is specified that prevents bedload transport from occurring up too steep an adverse slope.

Calibration of the Hydrodynamic and Sediment Transport Models

The same data sets used to calibrate the AQ hydrodynamic model (ADCP surveys conducted June 13 – July 7, 2010 and May 10 – July 13, 2011) were used to calibrate LTFATE. To date, the optimum agreement in the simulated and measured water levels and depth-averaged velocities was achieved using a globally averaged value of 0.1 cm for z_o = effective bed roughness that represents to total bottom roughness due to both skin friction and form drag. The RMS error in the water surface elevations for the 2010 and 2011 periods were 4.25 cm and 4.75 cm, respectively. The RMS error in the depth-averaged velocities for the 2010 and 2011 periods were 0.12 m/s and 0.11 m/s, respectively. Efforts to decrease these RMS errors are continuing. Likewise, the same data AQ used to calibrate their sediment transport model is being used to calibrate LTFATE, with the main metric being the net sedimentation rate. The calibration of the sediment transport model in LTFATE cannot be finalized until acceptable results are obtained from the hydrodynamic model calibration. The final results from these calibration efforts will be presented in the second report.

Task 4

Statement

Provide an uncertainty analysis of the model assumptions (flow rates, boundary representation, sediment transport, sedimentation rates, initial bed properties, etc.). Uncertainties should be clearly identified and assessed including sediment loads at the upstream Lake Houston Dam.

Findings

It is standard to evaluate the effects of uncertainties in model inputs using a sensitivity analysis. Thus, this task was performed by expanding on the sensitivity analyses performed by AQ with their models. A review of the analysis that AQ performed is given below, followed by a critique of their analysis, and then a description of the expanded sensitivity analysis being performed for this task is given.

1. AQ Sensitivity Analysis

The sensitivity analysis performed by AQ evaluated the effects of varying input parameters for both the sediment transport model and the hydrodynamic model. These analyses are summarized below.

The sensitivity analysis performed by AQ evaluated the effects of varying the following sediment transport model input parameters: erosion rates, incoming sediment load at the Lake Houston Dam, and the effective bed roughness as quantified by the value of D_{90}. The latter was only increased by a factor of two, whereas the incoming sediment load was varied by $\pm$ 2. Both changes are with respect to the base case simulation. Lower and upper-bound parameters that were based on the erosion rate ratio values for the Sedflume cores, with the lower-bound being Core SJSD010 and the upper-bound being Core SJSF003. AQ evaluated the effects of possible interactions among the three input parameters using a factorial analysis. The latter produced eight model simulations that accounted for all of the possible combinations of the upper and lower bounds of the three parameters. The results of these eight model simulations were compared "using the sediment mass balance for the Study Area as the metric for quantitative comparison". Figure 4-44 in Anchor QEA (2012) shows the predicted sediment mass balance for the entire model domain over the 21-year model simulation, and the trapping efficiency was determined to be

17 percent. Trapping efficiency is calculated as the percentage of the incoming sediment load that is deposited in the model domain. Seven of the eight sensitivity simulations had positive trapping efficiencies, i.e., they were net depositional over the 21-year simulation period, whereas one of the simulations was net erosional so no trapping efficiency was calculated for that simulation. The seven positive trapping efficiencies ranged from 6 to 24 percent (see Figure 4-49 in Anchor QEA (2012)). AQ also presents comparisons of the gross erosion rate, the gross deposition rate, and the rate of net change for the entire model domain and the Site Perimeter, respectively, in Figures 4-50 and 4-51 for the base case and eight sensitivity simulations. Their findings from these sensitivity simulations were the following: 1) Changes in the upstream sediment load had the largest effect on the net deposition over the 21-year simulation; and 2) The effects on both net erosion and net deposition due to the variations in erosion rate parameters and the effective bed roughness were of similar magnitude, and most importantly, were significantly less than the effect from varying the incoming sediment load from Lake Houston.

The sensitivity analysis performed by AQ evaluated the effects of varying the following hydrodynamic model input parameters: channel bathymetry in the vicinity of Grennel Slough, water inflow at the Lake Houston Dam, salinity at the downstream boundary, and the water surface elevation (WSE) at the downstream boundary. The effects of these input parameters on both the hydrodynamic and sediment transport models were determined by simulating conditions for 2008 (during which Hurricane Ike occurred) for both the base case (using the original input parameters) and the sensitivity model runs. The differences between the base case and the different sensitivity runs were quantified by determining the differences in bed elevation changes within the Site Perimeter at the end of the one-year model simulations. Results from this analysis are described next.

The channel bathymetry in the vicinity of Grennel Slough was modified by eliminating two areas that created a cutoff in the channel due to spatial interpolation of the bathymetric data. Analysis of the model simulation of 2008 found that the original bathymetry that contained the two cutoffs had negligible effect on the hydrodynamics and sediment transport within the Site.

As discussed in Anchor QEA (2012), the water releases at the Lake Houston Dam were estimated for the period of the 21-year simulation prior to July 1996. The impact of the method used to estimate the inflows into the SJR on the model results was evaluated by using the same method to estimate the inflows for 2008 and running the models for that year. The results from this analysis revealed that the method used for estimating the inflows prior to July 1996 had relatively minor effects on the sediment transport simulations within the Site perimeter.

A constant salinity of 16 psu was used at the downstream boundary for the 21-year simulations. The effect of the salinity value used for the downstream boundary on sediment transport simulations at the Site was investigated by simulating 2008 using both a salinity boundary condition of 16 and 0 psu. These two simulations were compared and negligible impacts on the sediment transport results were found. This is not a surprising result when using a depth-averaged model.

The effect of the WSE used at the downstream boundary was investigated in the following manner. The year 2002 was simulated using the WSE obtained from data collected at the Morgan's Point tidal gauge station as well as using the WSE data collected at the Battleship Texas State Park/Lynchburg station. The bed elevation changes for each grid cell within the Site Perimeter were compared between these two model simulations, and minimal differences were found. Thus, AQ concluded that the WSE data used at the downstream boundary in their model did not have a significant impact on the sediment transport results in proximity to the Site.

2. Critique of the AQ Sensitivity Analysis

Overall, the sensitivity analysis performed by AQ is the best method for attempting to put bounds on the uncertainty in results obtained from any transport and fate modeling study. The use of trapping efficiency as a metric for quantifying the results from the sensitivity analysis is thought to be somewhat limited in its usefulness. However, the finding that the largest source of uncertainty in the sediment transport modeling is the estimated sediment loading from the Lake Houston Dam is not surprising. As the USGS commented in their review, "to improve the model, better sediment load information from Lake Houston Dam is necessary." However, having more accurate sediment loading data may or may not

improve the model's ability to predict sediment transport in the SJR estuary. This same thought is conveyed in USGS's comments 29 and 37.

It is the opinion of the PDT that the largest source of uncertainty is the application of a model framework that does not account for morphologic feedback between the sediment transport and hydrodynamic models to a water body such as the SJR. The SJR estuary is subjected to aperiodic large hydrologic events, i.e., floods and hurricanes, such as the three significant events that occurred during the 21-year simulation period, during which significant sediment transport and large scale scour and sedimentation occurred in certain portions of the estuary. The unquantified uncertainty in applying a non-morphologic modeling system to such a system limits the usefulness of the sensitivity analysis performed using the non-morphologic models. In addition, the other issues discussed in Task 3, *e.g.*, inclusion of the 100-year floodplain in the model grid, location of the downstream boundary, definition used to classify sediment as cohesive, use of a hard bottom in the HSC, etc., are believed to further increase the uncertainty in the model results. A better model framework to use at the SJR would have been the one that AQ used in simulating primarily noncohesive sediment transport in the Tittabawassee River, Michigan in which a quasi-linkage routine was added between the sediment transport and hydrodynamic models. In both water bodies, the magnitude of the morphologic changes is within one order of magnitude of the water depths, thus necessitating the linkage between the hydrodynamic and sediment transport models.

3. Expanded Sensitivity Analysis

In an attempt to better quantify the uncertainty associated with the model framework and the other issues listed above and in Task 3, an expanded sensitivity analysis is being performed as a component of this project. It is being performed using the LTFATE modeling system that was setup to represent the SJR estuary model domain. The multiple model simulations are still underway at present, so no results are presented in this first report. The results will be included in the second report. A description of the methodology being used in performing this expanded sensitivity analysis is described next.

The effects of changes in the following parameters on model results are being investigated using a sensitivity analysis approach similar to the

factorial analysis methodology used by AQ with the LTFATE modeling system:

- Simulation of bedload
- Different classification of cohesive sediment
- Sediment loadings at the Lake Houston Dam
- Use of a non-hard bottom in the HSC

Table 2-1 lists the nine sensitivity simulations that have been setup and tested to insure there are no runtime errors for the different parameterizations. Run 1 represents the Base Case. Each of these sensitivity runs is for the September – October 1994 time period. The inclusion of the 100-year floodplain in the model grid and the use of the dynamically linked hydrodynamic model and sediment transport model option are being used in all nine sensitivity simulations.

Table 2-1
Sensitivity Simulations

Sensitivity Run	Bedload Simulated	Different cohesive sediment classification	Inflow sediment loadings	Hard bottom in the HSC
1	No	No	AQ	Yes
2	No	Yes	AQ	Yes
3	No	No	Upper Bound	Yes
4	No	No	Lower Bound	Yes
5	No	No	AQ	No
6	Yes	No	AQ	Yes
7	Yes	Yes	AQ	Yes
8	Yes	Yes	AQ	No
9	Yes	Yes	Upper Bound	No

Task 5 and Task 6

Statements

Perform a technical review of the design and construction of the entire existing cap as it is currently configured. Identify any recommended enhancements to the cap.

Assess the ability of the existing cap to prevent migration of dioxin, including diffusion and/or colloidal transport, through the cap with and without the geomembrane/geotextile present.

Findings

Background

Design and construction of the existing TCRA cap was divided into three sections, each of which has different cap components. The Western Cell is generally above the water line; the Eastern Cell is mostly covered with less than 5 ft (1.5 m) of water; and the Northwestern Area is mostly in greater than 10 ft (3.0 m) of water. The Western Cell cap is composed of a geotextile filter, a geomembrane, a protective geotextile cushion and armor stone. The Eastern Cell has a geotextile filter and armor stone. The Northwestern Area has predominantly granular filter blended with armor stone. These three sections were further subdivided into subsections with varying armor stone. The cap is presently built with some slopes steeper than 1V:3H. The thicknesses of the armor stone is at least twice the D_{50} of the stone. The armor stone is sized for limited movement during storm events having a return period of up to 100 years. The capped sediment consists predominantly of a soft, compressible, organically rich sludge.

Western Cell

The Western Cell should largely be physically stable provided that all surfaces have a slope flatter than 1V:3H, all areas of potential high bottom shear stress with a slope steeper than 1V:5H are covered in natural stone, the bottom shear stresses are properly modeled, and no significant localized deformations occur to disrupt the geomembrane. Soft sediments were solidified/stabilized prior to cap construction. The design and construction followed standard practice for land-based operations. The geotextiles were overlapped and geomembrane seams were welded. The

armor stone, geotextiles and geomembrane effectively isolates environmental receptors from the contaminated sediment. The geotextiles used in the design provide adequate protection for the geomembrane to prevent puncture and to provide long-term chemical isolation. The geomembrane will control infiltration, seepage and tidal pumping along with their associated dissolved and colloidal transport of contaminants. The geomembrane also controls diffusion and resuspension, effectively isolating the contaminants. No groundwater transport in the sediment under the cap across the site is anticipated based on the topography of the region, location of the site, and permeability of the sediment. Flattening of some steeper slopes is recommended to increase the factor of safety and provide for long-term stability.

Eastern Cell

The Eastern Cell should largely be physically stable provided that all surfaces have a slope flatter than 1V:3H, all areas of potential high bottom shear stress with a slope steeper than 1V:5H are covered in natural stone, the bottom shear stresses are properly modeled, and no significant localized deformations occur to disrupt the geotextile. The design and construction followed standard practice for water-side operations. The geotextiles were overlapped and secured in place during placement of the armor cap. The geotextiles were rolled out and advanced gradually during armor cap placement to maintain their positioning. The armor stone and geotextile effectively isolates environmental receptors from the contaminated sediment. The Eastern Cell does not contain a geomembrane to control resuspension and the advective and diffusive flux of contaminants. However, being submerged and relatively flat without regional surficial groundwater upwelling, no significant advective flux is anticipated to provide transport of dissolved or colloidal contaminants. A small quantity of porewater with dissolved and colloidal contaminants would be expelled in the short term through the cap from consolidation and compression of the sediment under the pressure loading imposed by the armor cap. This contaminant mass loss is very small compared to the resuspension losses prior to capping but likely to several times greater than the diffusive losses during the same period. Resuspension of contaminated particles is not expected because the geotextile will provide a filter to control particle movement and prevent translocation of the capped sediment to the surface. Therefore, contaminant transport is

restrictive to porewater expulsion and diffusion. The diffusive flux of contaminants from the capped area is very small compared to resuspension losses of contaminated particulates prior to capping; however, the diffusive losses from the sediment are largely unimpeded by the cap. The armor cap material does not have a significant quantity of organic carbon to retard contaminant transport. In addition, the large pore structure of the armor cap material would permit a large exchange of water within the cap, preventing the formation of a concentration gradient to slow the diffusion. Addition of an amendment like AquaGate™ or SediMite™ could further reduce the potential contaminant losses from diffusion. A product like AquaGate™ would also provide added protection from erosion by providing cohesion between granular particle and filling the pores of the Armor Cap C and D materials and perhaps also the recycled concrete of the Armor Cap A and B/C materials.

Northwestern Area

The design and construction of the cap in the Northwestern Area is very different than the other two cells and does not provide the same level of confidence in its long-term stability and performance. The area is largely capped with twelve inches of non-uniform recycled concrete blended with granular filter material at a ratio of 4:1. The D50 of the recycled concrete was specified to be 3 inches. Slopes within the Northwestern Area are as steep as 1V:2H. The cap was placed in layers proceeding from deep water to shallow water, following standard construction practices for water-side operations.

Placement of recycled concrete with a blended filter on slopes steeper than 1V:3H and perhaps as flat as 1V:5H slope promotes separation of the sand-sized particles and perhaps gravel-sized particles from the larger concrete particles. The finer particles would have a tendency to run down the slope, coarsening the cap on the upper portion of the slopes and reducing the effectiveness of the filter on the upper slope. Without a filter being placed on soft sediments (having low bearing capacity) prior to placement of the armor material, the larger particles of recycled concrete would embed themselves in the sediment and promote mixing of the cap with the sediment, limiting the isolation of the sediment. Use of a blended filter would tend to be less effective on very soft sediments than a separate granular filter. To ensure physical stability of the cap, the cap and blended

filter should be placed on a slope no greater than 1V:3H, and preferably 1V:5H.

Mixing of the sediment with the capping media and inadequate filtration due to loss of the finer fraction of the capping media (sands and perhaps gravel) due to separation during placement may allow losses by resuspension in addition to diffusion and porewater expulsion. Additionally, bioadvection of sediment may translocate sediment particles to the surface where the sediment can be resuspended. Burrowing to a depth of 12 to 15 inches (30.5 to 38.1 cm) may be expected in the absence of a geotextile or a geomembrane. Thickening the cap in the Northwestern Area would virtually eliminate the potential resuspension losses.

Regardless of whether resuspension losses occur, there are potential contaminant losses by diffusion, porewater expulsion, tidal pumping and groundwater seepage. Like the Eastern Cell, the Northwestern Area does not contain a geomembrane to control the advective and diffusive flux of contaminants. However, being submerged and relatively flat without regional surficial groundwater upwelling, no significant advective flux by groundwater seepage is anticipated to provide transport of dissolved or colloidal contaminants. A small quantity of porewater with dissolved and colloidal contaminants would be expelled in the short term through the cap from consolidation and compression of the sediment under the pressure loading imposed by the armor cap. This contaminant mass loss is very small compared to the resuspension losses prior to capping but likely to several times greater than the diffusive losses during the same period. Therefore, contaminant transport is restrictive to porewater expulsion and diffusion. The diffusive flux of contaminants from the capped area is very small compared to resuspension losses of contaminated particulates prior to capping; however, the diffusive losses from the sediment are largely unimpeded by the cap. The armor cap material does not have a significant quantity of organic carbon to retard contaminant transport. In addition, the large pore structure of the armor cap material would permit a large exchange of water within the cap by tidal pumping, preventing the formation of a concentration gradient to slow the diffusion. Addition of an amendment like AquaGate™ or SediMite™ could further reduce the potential contaminant losses from diffusion by the addition of activated carbon to sequester the contaminants and restrict the exchange of water within the cap. The activated carbon could provide in situ treatment of

sediment particles mixed into the cap during placement or bioadvected after placement, limiting resuspension losses as well as diffusion and advective losses from the cap. A product like AquaGate™ would also provide added protection from erosion by providing cohesion between granular particle and filling the pores of the recycled concrete of the Armor Cap A material.

References

Ackers, P. and W.R. White. 1973. Sediment transport: a new approach and analysis. *Journal of Hydraulic Engineering*, 99 (HY11).

Anchor QEA. 2012. "Chemical Fate and Transport Modeling Study San Jacinto River Waste Pits Superfund Site," Ocean Springs, MS.

Arega, F., and E.J. Hayter. 2008. Coupled Consolidation and Contaminant Transport Model for Simulating Migration of Contaminants through Sediment and a Cap. *Journal of Applied Mathematical Modelling*, 32, 2413–2428.

Bedient, 2013.

Brody, S.D., R. Blessing, K. Atoba, W. Mobley, and M. Wilson. 2014. "A Flood Risk Assessment of the San Jacinto River Waste Pit Superfund Site," Center for Texas Beaches and Shores, Texas A&M University, Galveston, TX.

Dyer, K.R. 1997. *Estuaries, A Physical Introduction*, 2nd Ed., John Wiley & Sons, New York.

Galperin, B., L.H. Kantha, S. Hassid, and A. Rosati. 1988. A quasi-equilibrium turbulent energy model for geophysical flows. *J. Atmos. Sci.,* **45**, 55-62.

Hamrick, J.M. 2007a. The Environmental Fluid Dynamics Code User Manual: US EPA Version 1.01. Tetra Tech, Inc., Fairfax, VA.

Hamrick, J.M. 2007b. The Environmental Fluid Dynamics Code Theory and Computation. Volume 1: Hydrodynamics and Mass Transport. Tetra Tech, Inc., Fairfax, VA.

Hamrick, J.M. 2007c. The Environmental Fluid Dynamics Code Theory and Computation. Volume 2: Sediment and Contaminant Transport and Fate. Tetra Tech, Inc., Fairfax, VA.

Hayter, E.J., and A.J. Mehta. 1986. "Modelling Cohesive Sediment Transport in Estuarial Waters." *Applied Mathematical Modelling*, 10(4), 294-303.

Hayter, E., J. Smith, D. Michalsen, Z. Demirbilek, and L. Lin. 2012. Dredged Material Placement Site Capacity Analysis for Navigation Improvement Project at Grays Harbor, WA. *ERDC/CHL Technical Report TR-08-13*. U.S. Army Engineer Research and Development Center, Vicksburg, MS,

Hayter, E.J., R.S. Chapman, P.V. Luong, S.J. Smith, D.B. Bryant. 2013. "Demonstration of Predictive Capabilities for Fine-Scale Sedimentation Patterns Within the Port of Anchorage, AK," Letter Report, U.S. Army Engineer Research and Development Center, Vicksburg, MS.

James, S.C., C.A. Jones, M.D. Grace, and J.D. Roberts. 2010. Advances in sediment transport modeling. *Journal of Hydraulic Research*, 48: 6, 754-763.

Jepsen, R., J. Roberts, A. Lucero, and M. Chapin. 2001. Canaveral ODMDS Dredged Material Erosion Rate Analysis. *Sand2001-1989*, Sandia National Laboratories, Albuquerque, NM.

Johnson, B.H. 1990. User's guide for models of dredged material disposal in open water. *Technical Report D-90-5*, U.S. Army Engineer Waterways Experiment Station, Vicksburg, MS.

Johnson, B.H., and M.T. Fong. 1995. Development and Verification of Numerical Models for Predicting the Initial Fate of Dredged Material Disposed in Open Water, Report 2: Theoretical Developments and Verification Results. *Technical Report DRP-93-1*, U.S. Engineer Waterways Experiment Station, Vicksburg, MS.

Jones, C.A., and W. Lick. 2001. SEDZLJ: A Sediment Transport Model. *Final Report*. University of California, Santa Barbara, California.

Krone, R.B. 1972. Field study of flocculation as a factor in estuarial shoaling processes. Technical Report No. 19, Committee on Tidal Hydraulics, U. S. Army Corps of Engineers, Vicksburg, MS.

Lick, W. 2009. *Sediment and Contaminant Transport in Surface Waters*, CRC Press, Boca Raton, FL.

McNeil, J., C. Taylor, and W. Lick. 1996. "Measurements of the erosion of undisturbed bottom sediments with depth." *Journal of Hydraulic Engineering*, 122(6), 316-324.

Mehta, A.J. 2014. *An introduction to hydraulics of fine sediment transport,* World Scientific.

Paaswell, R.E. 1973. "Causes and mechanisms of cohesive soil erosion: The state of the art." Special Report 135, Highway Research Board, Washington, DC, 52–74.

Partheniades, E. 1965. Erosion and deposition of cohesive soils. *Journal of Hydraulic Division*, ASCE, 91, 105–138.

Roberts, J.D., R.A. Jepsen, W. Lick. 1998. Effects of particle size and bulk density on erosion of quartz particles. *J. Hydraulic Engineering*, 124(12), 1261–1267.

Sanford, L.P. 2008. Modeling a dynamically varying mixed sediment bed with erosion, deposition, bioturbation, consolidation, and armoring. *Computers & Geosciences*, 34(10): 1263-1283.

Thanh, P.X.H., M.D. Grace, and S.C. James. 2008. Sandia National Laboratories Environmental Fluid Dynamics Code: Sediment Transport User Manual. *SAND2008-5621*. Sandia National Laboratories, Livermore, CA.

USGS. 1995. "Floods in Southeast Texas, October 1994," U.S. Geological Survey, Houston, TX.

Van Rijn, L.C. 1984. "Sediment Transport: part i: bedload transport; part ii: suspended load transport: part iii: bed forms and alluvial roughness." *Journal of Hydraulic Engineering,* 110(10), 1431-1456; 110(11), 1613-1641, 110(12), 1733-1754.

Appendix A

Description of LTFATE Modeling System

LTFATE is a multi-dimensional modeling system maintained by ERDC. The hydrodynamic module in LTFATE is the Environmental Fluid Dynamics Code (EFDC) surface water modeling system (Hamrick 2007a; 2007b; and 2007c). EFDC is a public domain, three-dimensional finite difference model that contains dynamically linked hydrodynamic and sediment transport modules. Brief descriptions of these two modules are described below.

Hydrodynamic module in LTFATE

EFDC can simulate barotropic and baroclinic flow in a water body due to astronomical tides, wind, density gradients, and river inflow. It solves the three-dimensional (3D), vertically hydrostatic, free surface, turbulence averaged equations of motion. EFDC is extremely versatile, and can be used for 1D, 2D-laterally averaged (*2DV*), 2D-vertically averaged (2DH), or 3D simulations of rivers, lakes, reservoirs, estuaries, coastal seas, and wetlands.

For realistic representation of horizontal boundaries, the governing equations in EFDC are formulated such that the horizontal coordinates, x and y, are curvilinear. To provide uniform resolution in the vertical direction, the sigma (stretching) transformation is used. The equations of motion and transport solved in EFDC are turbulence-averaged, because prior to averaging, although they represent a closed set of instantaneous velocities and concentrations, they cannot be solved for turbulent flows. A statistical approach is applied, where the instantaneous values are decomposed into mean and fluctuating values to enable the solution. Additional terms that represent turbulence are introduced to the equations for the mean flow. Turbulent equations of motion are formulated to utilize the Boussinesq approximation for variable density. The Boussinesq approximation accounts for variations in density only in the gravity term. This assumption simplifies the governing equations significantly, but may introduce large errors when density gradients are large.

The resulting governing equations, presented in Appendix B, include parameterized, Reynolds-averaged stress and flux terms that account for the turbulent diffusion of momentum, heat and salt. The turbulence parameterization in EFDC is based on the Mellor and Yamada (1982) level 2.5 turbulence closure scheme, as modified by Galperin *et al.* (1988), that relates turbulent correlation terms to the mean state variables. The EFDC model also solves several transport and transformation equations for different dissolved and suspended constituents, including suspended sediments, toxic contaminants, and water quality state variables. Detailed descriptions of the model formulation and numerical solution technique used in EFDC are provided by Hamrick (2007b). Additional capabilities of EFDC include: 1) simulation of wetting and drying of flood plains, mud flats, and tidal marshes; 2) integrated, near-field mixing zone model; 3) simulation of hydraulic control structures such as dams and culverts; and 4) simulation of wave boundary layers and wave-induced mean currents. A more detailed description of EFDC is given in Appendix B.

Sediment transport module

The sediment transport model in LTFATE is a modified version of the SEDZLJ mixed sediment transport model (Jones and Lick 2001; James *et al.* 2010) that a) includes a three-dimensional representation of the sediment bed, and b) can simulate winnowing and armoring of the surficial layer of the sediment bed. SEDZLJ is dynamically linked to LTFATE in that the hydrodynamics and sediment transport modules are both run during each model time step. This enables simulated changes in morphology to be instantly fed-back to the hydrodynamic model. A more detailed description of SEDZLJ is given in Appendix C.

One of the first steps in performing sediment transport modeling is to use grain size distribution data from sediment samples collected at different locations throughout the model domain to determine how many discrete sediment size classes are needed to adequately represent the full range of sediment sizes. Typically, three to eight size classes are used. For example, AQ used four sediment size classes in their sediment transport model of the SJR. One size class was used to represent sediment in the cohesive sediment size range, 5 μm, and three size classes were used to represent the noncohesive sediment size range, 140, 510 and 3,500 μm.

Appendix B

Description of LTFATE Hydrodynamic Module

EFDC is a public domain, 3D finite difference model that contains dynamically linked hydrodynamic and sediment transport modules. EFDC can simulate barotropic and baroclinic flow in a water body due to astronomical tides, wind, density gradients, and river inflow. It solves the 3D vertically hydrostatic, free surface, turbulence averaged equations of motion. EFDC can be used for 1D, 2D-laterally averaged (*2DV*), 2D-vertically averaged (2DH), or 3D simulations of rivers, lakes, reservoirs, estuaries, coastal seas, and wetlands.

EFDC solves the 3D Reynolds-averaged equations of continuity (Equation B-1), linear momentum (Equations B-2 and B-3), hydrostatic pressure (Equation B-4), equation of state (Equation B-5) and transport equations for salinity and temperature (Equations B-6 and B-7) written for curvilinear-orthogonal horizontal coordinates and a sigma (stretching) vertical coordinate. These are given by Hamrick (2007b) and repeated below:

$$\frac{\partial(m\varepsilon)}{\partial t}+\frac{\partial(m_y Hu)}{\partial x}+\frac{\partial(m_x Hv)}{\partial y}+\frac{\partial(mw)}{\partial z}=0 \qquad \text{(B-1)}$$

$$\frac{\partial(mHu)}{\partial t}+\frac{\partial(m_y Huu)}{\partial x}+\frac{\partial(m_x Hvu)}{\partial y}+\frac{\partial(mwu)}{\partial z}-$$
$$(mf+v\frac{\partial(m_y)}{\partial x}-u\frac{\partial m_x}{\partial y})Hv=m_y H\frac{\partial(g\varepsilon+p)}{\partial x}- \qquad \text{(B-2)}$$
$$m_y(\frac{\partial H}{\partial x}-z\frac{\partial H}{\partial x})\frac{\partial p}{\partial z}+\frac{\partial(mH^{-1}A_v\frac{\partial u}{\partial z})}{\partial z}+Q_u$$

$$\frac{\partial(mHv)}{\partial t}+\frac{\partial(m_yHuv)}{\partial x}+\frac{\partial(m_xHvv)}{\partial y}+\frac{\partial(mwv)}{\partial z}+$$
$$(mf+v\frac{\partial(m_y)}{\partial x}+u\frac{\partial m_x}{\partial y})Hu=m_xH\frac{\partial(g\varepsilon+p)}{\partial y}- \quad \text{(B-3)}$$
$$m_x(\frac{\partial H}{\partial y}-z\frac{\partial H}{\partial y})\frac{\partial p}{\partial z}+\frac{\partial(mH^{-1}A_v\frac{\partial v}{\partial z})}{\partial z}+Q_v$$

$$\frac{\partial p}{\partial z}=\frac{gH(\rho-\rho_o)}{\rho_o}=gHb \quad \text{(B-4)}$$

$$\rho=\rho\ \rho,S,T \quad \text{(B-5)}$$

$$\frac{\partial(mHS)}{\partial t}+\frac{\partial(m_yHuS)}{\partial x}+\frac{\partial(m_xHvS)}{\partial y}+\frac{\partial(mwS)}{\partial z}=\frac{\partial(\frac{mA_b}{H}\frac{\partial S}{\partial z})}{\partial z}+Q_s \quad \text{(B-6)}$$

$$\frac{\partial(mHT)}{\partial t}+\frac{\partial(m_yHuT)}{\partial x}+\frac{\partial(m_xHvT)}{\partial y}+\frac{\partial(mwT)}{\partial z}=\frac{\partial(\frac{mA_b}{H}\frac{\partial T}{\partial z})}{\partial z}+Q_T \quad \text{(B-7)}$$

where u and v are the mean horizontal velocity components in (x,y) coordinates; m_x and m_y are the square roots of the diagonal components of the metric tensor, and $m= m_x\, m_y$ is the Jacobian or square root of the metric tensor determinant; p is the pressure in excess of the reference pressure, $\frac{\rho_o gH(1-z)}{\rho_o}$, where ρ_o is the reference density; f is the Coriolis parameter for latitudinal variation; A_v is the vertical turbulent viscosity; and A_b is the vertical turbulent diffusivity. The buoyancy b in Equation B-4 is the normalized deviation of density from the reference value. Equation B-5 is the equation of state that calculates water density, ρ, as functions of p, salinity, S, and temperature, T.

The sigma (stretching) transformation and mapping of the vertical coordinate is given as:

$$z=\frac{(z^*+h)}{(\xi+h)} \quad \text{(B-8)}$$

where z^* is the physical vertical coordinate, and h and ξ are the depth below and the displacement about the undisturbed physical vertical coordinate origin, $z^* = 0$, respectively, and $H=h+\xi$ is the total depth. The vertical velocity in z coordinates, w, is related to the physical vertical velocity w^* by:

$$w = w^* - z(\frac{\partial \xi}{\partial t} + \frac{u}{m_x}\frac{\partial \xi}{\partial x} + \frac{v}{m_y}\frac{\partial \xi}{\partial y}) + (1-z)(\frac{u}{m_x}\frac{\partial h}{\partial x} + \frac{v}{m_y}\frac{\partial h}{\partial y}) \qquad \text{(B-9)}$$

The solutions of Equations B-2, B-3, B-6 and B-7 require the values for the vertical turbulent viscosity and diffusivity and the source and sink terms. The vertical eddy viscosity and diffusivity, A_v and A_b, are parameterized according to the level 2.5 (second-order) turbulence closure model of Mellor and Yamada (1982), as modified by Galperin *et al.* (1988), in which the vertical eddy viscosities are calculated based on the turbulent kinetic energy and the turbulent macroscale equations. The Mellor and Yamada level 2.5 (MY2.5) turbulence closure model is derived by starting from the Reynolds stress and turbulent heat flux equations under the assumption of a nearly isotropic environment, where the Reynolds stress is generated due to the exchange of momentum in the turbulent mixing process. To make the turbulence equations closed, all empirical constants are obtained by assuming that turbulent heat production is primarily balanced by turbulent dissipation.

The vertical turbulent viscosity and diffusivity are related to the turbulent intensity, q^2, turbulent length scale, l and a Richardson number R_q as follows:

$$A_v = \Phi_v q l = 0.4(1+36R_q)^{-1}(1+6R_q)^{-1}(1+8R_q)ql \qquad \text{(B-10)}$$

$$A_b = \Phi_b q l = 0.5(1+36R_q)^{-1} ql \qquad \text{(B-11)}$$

where A_v and A_b are stability functions that account for reduced and enhanced vertical mixing or transport in stable and unstable vertical, density-stratified environments, respectively, and the local Richardson number is given as:

$$R_q = \frac{gH\dfrac{\partial b}{\partial z}}{q^2}\frac{l^2}{H^2} \qquad \text{(B-12)}$$

A critical Richardson number, R_q = 0.20, was found at which turbulence and mixing cease to exist (Mellor and Yamada 1982). Galperin *et al.* (1988) introduced a length scale limitation in the MY scheme by imposing an upper limit for the mixing length to account for the limitation of the vertical turbulent excursions in stably stratified flows. They also modified and introduced stability functions that account for reduced or enhanced vertical mixing for different stratification regimes.

The turbulence intensity (q^2) and the turbulence length scale (l) are computed using the following two transport equations:

$$\frac{\partial(mHq^2)}{\partial t}+\frac{\partial(m_y Huq^2)}{\partial x}+\frac{\partial(m_x Hvq^2)}{\partial y}+\frac{\partial(mwq^2)}{\partial z}=\frac{\partial(\dfrac{mA_q\dfrac{\partial q^2}{\partial z}}{H})}{\partial z}+Q_q \qquad \text{(B-13)}$$
$$+2\frac{mA_v}{H}((\frac{\partial^2 u}{\partial z^2})+(\frac{\partial^2 v}{\partial z^2}))+2mgA_b\frac{\partial b}{\partial z}-2mH(\frac{q^3}{(B_1 l)})$$

$$\frac{\partial(mHq^2 l)}{\partial t}+\frac{\partial(m_y Huq^2 l)}{\partial x}+\frac{\partial(m_x Hvq^2 l)}{\partial y}+\frac{\partial(mwq^2 l)}{\partial z}=$$
$$\frac{\partial(\dfrac{mA_q\dfrac{\partial q^2 l}{\partial z}}{H})}{\partial z}+Q_l+2\frac{mE_1 lA_v}{H}((\frac{\partial^2 u}{\partial z^2})+(\frac{\partial^2 v}{\partial z^2}))+mgE_1E_3lA_b\frac{\partial b}{\partial z} \qquad \text{(B-14)}$$
$$-H(\frac{q^3}{(B_1)})(1+E_2(\kappa L)^{-2}l^2)$$

The above two equations include a wall proximity function, $W=1+E_2 l(\kappa L)^{-2}$, that assures a positive value of diffusion coefficient $L^{-1}=(H)^{-1}(z^{-1}+(1-z)^{-1}))$. κ, B_1, E_1, E_2, and E_3 are empirical constants with values 0.4, 16.6, 1.8, 1.33, and 0.25, respectively. All terms with *Q's* (Q_u, Q_v, Q_q, Q_l, Q_s, Q_T) are sub-grid scale sink-source terms that are modeled as sub-grid scale horizontal diffusion. The vertical diffusivity, A_q, is in general taken to be equal to the vertical turbulent viscosity, A_v (Hamrick 2007b).

The vertical boundary conditions for the solutions of the momentum equations are based on the specification of the kinematic shear stresses. At the bottom, the bed shear stresses are computed using the near bed velocity components (u_1,v_1) as:

$$(\tau_{bx},\tau_{by}) = c_b\sqrt{u_1^2+v_1^2}(u_1,v_1) \qquad \text{(B-15)}$$

where the bottom drag coefficient $c_b = (\frac{\kappa}{\ln(\Delta_1/2z_o)})^2$, where κ is the von Karman constant, Δ_1 is the dimensionless thickness of the bottom layer, $z_o = z_o^*/H$ is the dimensionless roughness height, and z_o^* is roughness height in meters. At the surface layer, the shear stresses are computed using the u, v components of the wind velocity (u_w,v_w) above the water surface (usually measured at 10 m above the surface) and are given as:

$$(\tau_{sx},\tau_{sy}) = c_s\sqrt{u_w^2+v_w^2}(u_w,v_w) \qquad \text{(B-16)}$$

where $c_s = 0.001\frac{\rho_a}{\rho_w}(0.8+0.065\sqrt{u_w{}^2+v_w^2})$ and ρ_a and ρ_w are the air and water densities, respectively. Zero flux vertical boundary conditions are used for the transport equations.

Numerically, EFDC is second-order accurate both in space and time. A staggered grid or C-grid provides the framework for the second-order accurate spatial finite differencing used to solve the equations of motion. Integration over time involves an internal-external mode splitting procedure separating the internal shear, or baroclinic mode, from the external free surface gravity wave, or barotropic mode. In the external mode, the model uses a semi-implicit scheme that allows the use of relatively large time steps. The internal equations are solved at the same time step as the external equations, and are implicit with respect to vertical diffusion. Details of the finite difference numerical schemes used in the EFDC model are given in Hamrick (2007b), and will not be presented in this report.

The generic transport equation solved in EFDC for a dissolved (*e.g.*, chemical contaminant) or suspended (*e.g.*, sediment) constituent having a mass per unit volume concentration C, is

$$\frac{\partial m_x m_y HC}{\partial t}+\frac{\partial m_y HuC}{\partial_x}+\frac{\partial m_x HvC}{\partial y}+\frac{\partial m_x m_y wC}{\partial z}-\frac{\partial m_x m_y w_{sc} C}{\partial z}=$$
$$\frac{\partial}{\partial_x}\left(\frac{m_y}{m_x}HK_H\frac{\partial C}{\partial x}\right)+\frac{\partial}{\partial_y}\left(\frac{m_x}{m_y}HK_H\frac{\partial C}{\partial y}\right)+\frac{\partial}{\partial_z}\left(m_x m_y\frac{K_v}{H}\frac{\partial C}{\partial z}\right)+Q_c \quad \text{(B-17)}$$

where K_V and K_H are the vertical and horizontal turbulent diffusion coefficients, respectively; w_{sc} is a positive settling velocity when C represents the mass concentration of suspended sediment; and Q_c represents external sources or sinks and reactive internal sources or sinks. For sediment, $C = S_i$, where S_i represents the concentration of the *ith* sediment class. So, Eq. B-17, which is the 3D advective-dispersive transport equation, is solved for each of the sediment size classes that the grain size distribution at the site is divided into. In this case, Q_{ci} = source/sink term for the *ith* sediment size class that accounts for erosion/deposition. The equation used to calculate Q_{ci} is the following:

$$S_i = E_{sus,i} - D_{sus,i} \quad \text{(B-18)}$$

where $E_{sus,i}$ = sediment erosion rate for the *ith* sediment size class that is eroded and entrained into suspension, and $D_{sus,i}$ = sediment deposition rate for the *ith* sediment size class. Expressions for $D_{sus,i}$ and $E_{sus,i}$ are given later in this chapter.

The solution procedure for Eq. B-17 is the same as that for the salinity and heat transport equations, which use a high-order upwind difference solution scheme for the advection terms (Hamrick 2007b). Although the advection scheme is designed to minimize numerical diffusion, a small amount of horizontal diffusion remains inherent in the numerical scheme. As such, the horizontal diffusion terms in Equation B-17 are omitted by setting K_H equal to zero.

Appendix B

Description of LTFATE Sediment Transport Module

The sediment transport model in LTFATE is a modified version of the SEDZLJ mixed sediment transport model (Jones and Lick 2001; James *et al.* 2010) that includes a 3D representation of the sediment bed, and can simulate winnowing and armoring of the surficial layer of the sediment bed. SEDZLJ is dynamically linked to LTFATE in that the hydrodynamic and sediment transport modules are both run during each model time step.

Suspended Load Transport of Sediment

LTFATE solves Equation B-17 for the transport of each of the sediment classes to determine the suspension concentration for each size class in every water column layer in each grid cell. Included in this equation is the settling velocity, $w_{sc,}$ for each sediment size class. The settling velocities for noncohesive sediments are calculated in SEDZLJ using the following equation (Cheng 1997):

$$W_s = \frac{\mu}{d}\left(\sqrt{25+1.2d_*^2}-5\right)^{\frac{3}{2}} \quad \text{(C-1)}$$

where μ = dynamic viscosity of water; d = sediment diameter; and d_* = non-dimensional particle diameter given by:

$$d_* = d\left[\left(\rho_s/\rho_w - 1\right)g/\nu^2\right]^{1/3} \quad \text{(C-2)}$$

where ρ_w = water density, ρ_s = sediment particle density, g = acceleration due to gravity, and ν = kinematic fluid viscosity. Cheng's formula is based on measured settling speeds of real sediments. As a result it produces slower settling speeds than those given by Stokes' Law because real sediments have irregular shapes and thus a greater hydrodynamic resistance than perfect spheres as assumed in Stokes' law.

For the cohesive sediment size classes, the settling velocities are set equal to the mean settling velocities of flocs and eroded bed aggregates determined from an empirical formulation that is a function of the concentration of suspended sediment.

The erosion and deposition of each of the sediment size classes, *i.e.*, the source/sink term in the 3D transport equation (Equation C-17), and the subsequent change in the composition and thickness of the sediment bed in each grid cell are calculated by SEDZLJ at each time step.

Description of SEDZLJ

The sediment bed model in LTFATE is the SEDZLJ sediment transport model (Jones and Lick 2001). SEDZLJ is dynamically linked to EFDC in LTFATE. SEDZLJ is an advanced sediment bed model that represents the dynamic processes of erosion, bedload transport, bed sorting, armoring, consolidation of fine-grain sediment dominated sediment beds, settling of flocculated cohesive sediment, settling of individual noncohesive sediment particles, and deposition. An active layer formulation is used to describe sediment bed interactions during simultaneous erosion and deposition. The active layer facilitates coarsening during the bed armoring process.

Figure C-1 shows the simulated sediment transport processes in SEDZLJ. In this figure, U = near bed flow velocity, δ_{bl} = thickness of layer in which bedload occurs, U_{bl} = average bedload transport velocity, D_{bl} = sediment deposition rate for the sediment being transported as bedload E_{bl} = sediment erosion rate for the sediment being transported as bedload, E_{sus} = sediment erosion rate for the sediment that is eroded and entrained into suspension, and D_{sus} = sediment deposition rate for suspended sediment. Specific capabilities of SEDZLJ are listed below.

- Whereas a hydrodynamic model is calibrated to account for the total bed shear stress, which is the sum of the form drag due to bed forms and other large-scale physical features and the skin friction (also called the surface friction), the correct component of the bed shear stress to

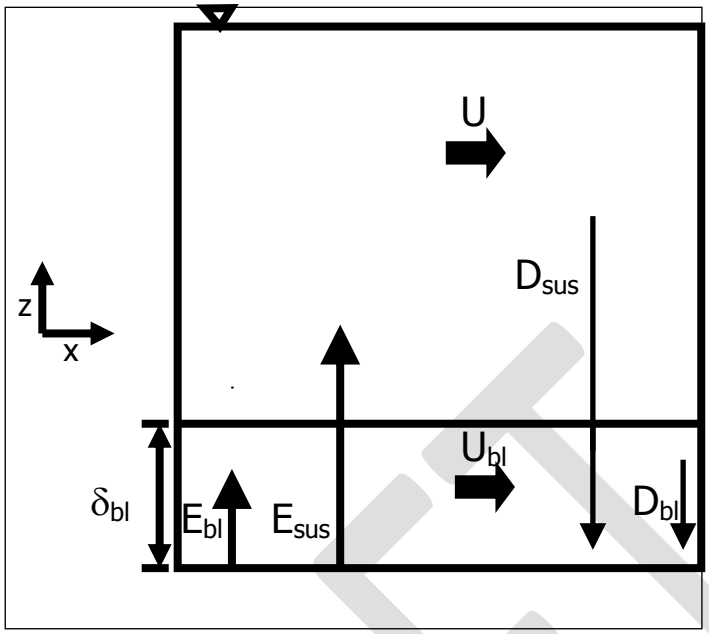

Figure C-1. Sediment transport processes simulated in SEDZLJ.

use in predicting sediment resuspension and deposition is the skin friction. The skin friction is calculated in SEDZLJ as a function of the near-bed current velocity and the effective bed roughness. The latter is specified in SEDZLJ as a linear function of the mean particle diameter in the active layer.

Multiple size classes of both fine-grain (*i.e.*, cohesive) and noncohesive sediments can be represented in the sediment bed. As stated previously, this capability is necessary to simulate coarsening and subsequent armoring of the surficial sediment bed surface during high flow events.

- To correctly represent the processes of erosion and deposition, the sediment bed in SEDZLJ can be divided into multiple layers, some of which are used to represent the existing sediment bed and others that are used to represent new bed layers that form due to deposition during model simulations. Figure C-2 shows a schematic diagram of this multiple bed layer structure. The graph on the right hand side of this figure shows the variation in the measured gross erosion rate (in units of *cm/s*) with depth into the sediment bed as a function of the applied skin

friction. A SEDFLUME study is normally used to measure these erosion rates.

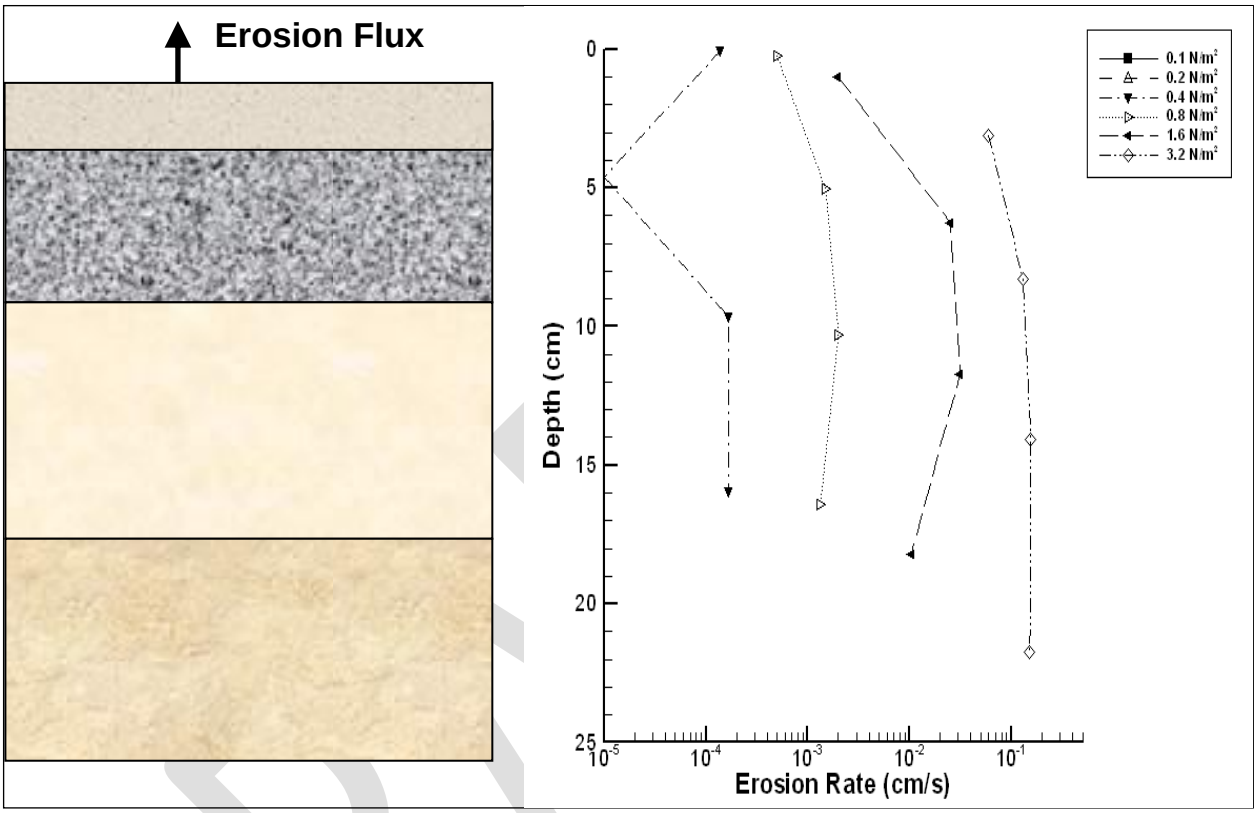

Figure C-2. Multi-bed layer model used in SEDZLJ.

- Erosion from both cohesive and non-cohesive beds is affected by bed armoring, which is a process that limits the amount of bed erosion that occurs during a high-flow event. Bed armoring occurs in a bed that contains a range of particle sizes (*e.g.*, clay, silt, sand). During a high-flow event when erosion is occurring, finer particles (*i.e.*, clay and silt, and fine sand) tend to be eroded at a faster rate than coarser particles (*i.e.*, medium to coarse sand). The differences in erosion rates of the various sediment particle sizes creates a thin layer at the surface of the sediment bed, referred to as the active layer, that is depleted of finer particles and enriched with coarser particles. This depletion-enrichment process can lead to bed armoring, where the active layer is primarily composed of coarse particles that have limited mobility. The multiple bed model in SEDZLJ accounts for the exchange of sediment through and the change in composition of this active layer. The thickness of the active layer is normally calculated as a time varying function of the mean

sediment particle diameter in the active layer, the critical shear stress for resuspension corresponding to the mean particle diameter, and the bed shear stress. Figure C-3 shows a schematic of the active layer at the top of the multi-bed layer model used in SEDZLJ.

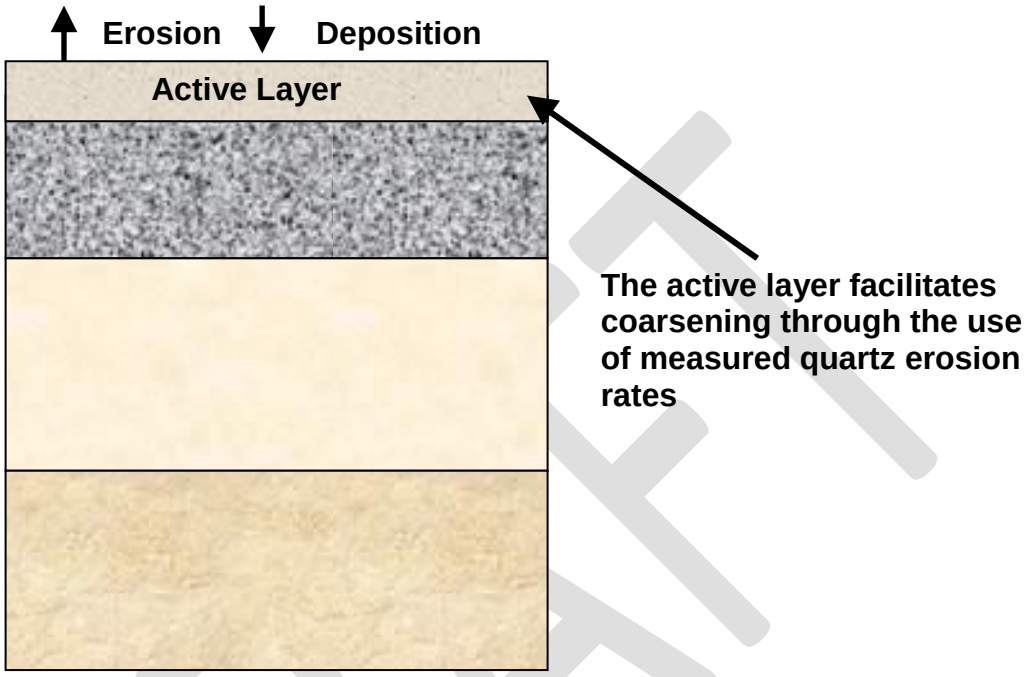

Figure C-3. Schematic of Active Layer used in SEDZLJ.

- SEDZLJ was designed to use the results obtained with SEDFLUME, which is a straight, closed conduit rectangular cross-section flume in which detailed measurements of critical shear stress of erosion and erosion rate as a function of sediment depth are made using sediment cores dominated by cohesive sediment collected at the site to be modeled (McNeil *et al.* 1996). However, when SEDFLUME results are not available, it is possible to use a combination of values for these parameters available from literature and/or the results of SEDFLUME tests performed at other similar sites. In this case, a detailed sensitivity analysis should be performed to assist in quantifying the uncertainty that results from the use of these non-site specific erosion parameters.

- SEDZLJ can simulate overburden-induced consolidation of cohesive sediments. An algorithm that simulates the process of primary consolidation, which is caused by the expulsion of pore water from the

sediment, of a fine-grained, *i.e.*, cohesive, dominated sediment bed is included in SEDZLJ. The consolidation algorithm in SEDZLJ accounts for the following changes in two important bed parameters: 1) increase in bed bulk density with time due to the expulsion of pore water, and 2) increase in the bed shear strength (also referred to as the critical shear stress for resuspension) with time. The latter parameter is the minimum value of the bed shear stress at which measurable resuspension of cohesive sediment occurs. As such, the process of consolidation typically results in reduced erosion for a given excess bed shear stress (defined as the difference between the bed shear stress and the critical shear stress for erosion) due to the increase in the bed shear strength. In addition, the increase in bulk density needs to be represented to accurately account for the mass of sediment (per unit bed area) that resuspends when the bed surface is subjected to a flow-induced excess bed shear stress.

Models that represent primary consolidation range from empirical equations that approximate the increases in bed bulk density and critical shear stress for resuspension due to porewater expulsion (Sanford 2008) to finite difference models that solve the non-linear finite strain consolidation equation that governs primary consolidation in saturated porous media (*e.g.*, Arega and Hayter 2008). An empirical-based consolidation algorithm is included in SEDZLJ.

- SEDZLJ contains a morphologic algorithm that, when enabled by the model user, will adjust the bed elevation to account for erosion and deposition of sediment.

Bedload Transport of Noncohesive Sediment

The approach used by Van Rijn (1984) to simulate bedload transport is used in SEDZLJ. The 2D mass balance equation for the concentration of sediment moving as bedload is given by:

$$\frac{\partial\left(\delta_{bl}C_b\right)}{\partial t} = \frac{\partial q_{b,x}}{\partial x} + \frac{\partial q_{b,y}}{\partial y} + Q_b \qquad \text{(C-3)}$$

where δ_{bl} = bedload thickness; C_b = bedload concentration; $q_{b,x}$ and $q_{b,y}$ = x- and y-components of the bedload sediment flux, respectively; and Q_b =

sediment flux from the bed. Van Rijn (1984) gives the following equation for the thickness of the layer in which bedload is occurring:

$$\delta_{bl} = 0.3 d d_*^{0.7} (\Delta\tau)^{0.5} \tag{C-4}$$

where $\Delta\tau = \tau_b - \tau_{ce}$; τ_b = bed shear stress, and τ_{ce} = critical shear stress for erosion.

The bedload fluxes in the *x*- and *y*-directions are given by:

$$q_{b,x} = \delta_{bl} u_{b,x} C_b$$

$$q_{b,y} = \delta_{bl} u_{b,y} C_b$$

where $u_{b,x}$ and $u_{b,y}$ = *x*- and *y*-components of the bedload velocity, u_b, which van Rijn (1984) gave as

$$u_b = 1.5 \tau_*^{0.6} \left[\left(\frac{\rho_s}{\rho_w} - 1 \right) g d \right]^{0.5} \tag{C-5}$$

with the dimensionless parameter τ_* given as

$$\tau_* = \frac{\tau_b - \tau_{ce}}{\tau_{ce}} \tag{C-6}$$

The *x*- and *y*-components of u_b are calculated as the vector projections of the LTFATE Cartesian velocity components *u* and *v*.

The sediment flux from the bed due to bedload, Q_{bl}, is equal to

$$Q_b = E_{bl} - D_{bl} \tag{C-7}$$

Deposition of Sediment

In contrast to previous conceptual models, deposition of suspended noncohesive sediment and cohesive flocs is now believed to occur continually, and not just when the bed shear stress is less than a so-called critical shear stress of deposition (Mehta 2014). The rate of deposition of the *ith* sediment size class, $D_{sus,i}$ is given by:

$$D_{sus,i} = -\frac{W_{s,i} C_i}{d} \tag{C-8}$$

where $W_{s,i}$ is given by Eq. C-1 for noncohesive sediment and by the empirical formulation used for the settling velocities of suspended flocs and bed aggregates, and d = thickness of the bottom water column layer in a three-dimensional model. Because of their high settling velocities, noncohesive sediments deposit relatively quickly (in comparison to the deposition of cohesive sediments) under all flows. Due to the settling velocities of flocs being a lot slower than those of noncohesive sediment, the deposition rate of flocs are usually several orders of magnitude smaller.

Deposited cohesive sediments usually form a thin surface layer that is often called a fluff or benthic nepheloid layer that is often less than 1 cm in thickness. The fluff layer typically forms in estuaries and coastal waters via deposition of suspended flocs during the decelerating phase of tidal flows, in particular immediately before slack water (Krone 1972; and Hayter and Mehta 1986). The fluff layer is usually easily resuspended by the accelerating currents following slack water in tidal bodies of water.

The rate of deposition of the *ith* noncohesive sediment class moving as bedload is given by (James *et al.* 2010):

$$D_{bl,i} = -P_{bl,i} W_{s,i} C_{bl,i} \tag{C-9}$$

where $C_{bl,i}$ = mass concentration of the *ith* noncohesive sediment class being transported as bedload, and $P_{bl,i}$ = probability of deposition from bedload transport. The latter parameter is given by:

$$P_{bl,i} = \frac{E_{bl,i}}{W_{s,i} C_{bl,i}^{eq}} \tag{C-10}$$

where

$$C_{bl,i}^{eq} = \frac{0.18 C_o \tau_b}{d_*} \tag{C-11}$$

which is the steady-state sediment concentration in bedload that results from a dynamic equilibrium between erosion and deposition, d_* is given by Eq. C-2, and C_o = 0.65.

Erosion of Sediment

Erosion of a cohesive sediment bed occurs whenever the current and wave-induced bed shear stress is great enough to break the electrochemical interparticle bonds (Partheniades 1965; Paaswell 1973). When this happens, erosion takes place by the removal of individual sediment particles or bed aggregates. This type of erosion is time dependent and is defined as surface erosion or resuspension. In contrast, another type of erosion occurs more or less instantaneously by the removal of relatively large pieces of the bed. This process is referred to as mass erosion, and occurs when the bed shear stress exceeds the bed bulk strength along some deep-seated plane that is typically much greater than the bed shear strength of the surficial sediment.

The erosion rate of cohesive sediments, E, is given experimentally by:

$$\begin{aligned} E &= 0; && (\tau < \tau_{cr}) \\ E &= A\tau^n; && (\tau_{cr} < \tau < \tau_m) \\ E &= A\tau_m^n; && (\tau > \tau_m) \end{aligned} \qquad \text{(C-12)}$$

where the exponent, coefficient, critical shear stress for erosion, and maximum shear stress (above which E is not a function of τ) n, A, and τ_{cr}, respectively, are determined from a SEDFLUME study. The erosion rates of the noncohesive sediment size classes were determined as a function of the difference between the bed shear stress and the critical shear stress for erosion using the results obtained by Roberts *et al.* (1998) who measured the erosion rates of quartz particles in a SEDFLUME.

The erosion rate of the *ith* noncohesive sediment size class that is transported as bedload, $E_{bl,i}$, is calculated by the following equation in which it is assumed there is dynamic equilibrium between erosion and deposition:

$$E_{bl,i} = P_{bl,i} W_{s,i} C_{bl,i} \qquad \text{(C-13)}$$